Biotransformation of hexachlorocyclohexanes contaminated biomass for energetic utilization demonstrated in continuous anaerobic digestion system

Shujuan Lian[a], Marcell Nikolausz*[b], Ivonne Nijenhuis[a], Ulisses Nunes da Rocha[b], Bin Liu[b], Felipe Borim Corrêa[b], João Pedro Leonor Fernandes Saraiva[b] and Hans Hermann Richnow*[a]

[a] Department of Isotope Biogeochemistry, Helmholtz Centre for Environmental Research - UFZ, Permoserstraße 15, 04318 Leipzig, Germany
(E-mail: shujuan.lian@ufz.de, ivonne.nijenhuis@ufz.de, hans.richnow@ufz.de)

[b] Department of Environmental Microbiology, Helmholtz Centre for Environmental Research - UFZ, Permoserstraße 15, 04318 Leipzig, Germany
(E-mail: marcell.nikolausz@ufz.de, ulisses.rocha@ufz.de, bin.liu@ufz.de, felipe.correa@ufz.de, joao.saraiva@ufz.de)

*Corresponding authors:

Hans Hermann Richnow, Tel.: +49 341 2351 212; E-mail: hans.richnow@ufz.de

Marcell Nikolausz, Tel.: +49 341 243 4566; E-mail: marcell.nikolausz@ufz.de

Abstract

Lindane, the γ-hexachlorocyclohexane (HCH) isomer, was among the most used pesticides worldwide. Although it was banned in 2009, residues of Lindane and other HCH-isomers are still found with high concentrations in contaminated fields. For clean-up, phytoremediation combined with anaerobic digestion (AD) of contaminated biomass to produce biogas and fertilizer could be a promising strategy and was tested in two 15 L laboratory-scale continuous-stirred-tank-reactors. During operation over one year by adding HCH isomers (γ, α and β) consecutively, no negative influence on conventional reactor parameters was observed. The γ- and α-HCH isomers were transformed to chlorobenzene and benzene, and transformation became faster along with time, while β-HCH was not removed. Genus *Methanosaeta* and order *Clostridiales*, showing significant enhancement on abundance with HCH addition, may be used as bioindicators for HCH dehalogenation in AD process. The potential for HCH degradation in AD system was restricted to axial Cl atoms of HCH and it showed slight enantioselective preference towards transformation of (+) α-HCH. Moreover, metabolite benzene was mineralized to CO_2 and methane, deducing from tracer experiments with benzene-$^{13}C_6$. Overall, AD appears to be a feasible option for treatment of γ and α-HCHs contaminated biomass.

Key words: Hexachlorocyclohexane; anaerobic digestion; stable isotope; reductive dehalogenation; cleanup strategy

1. Introduction

Contamination by Persistent Organic Pollutants (POPs) prevents further utilization of arable lands for food and feed production. However, such lands may still be utilized for growth of energy crops with degradation properties such as wheat or other plants [1,2]. Potentially the contaminated biomass can be used as feedstock for anaerobic digestion (AD) to produce biogas as energy carrier and for use of the digestate as fertilizer. Thus, we propose a strategy combing phytoremediation with AD of hexachlorocyclohexane (HCH) contaminated biomass to produce biogas and still retain soil fertility, which might be a model for other halogenated POPs.

Huge amounts of Lindane, γ-HCH, have been used as pesticide worldwide until banned in the Stockholm convention 2009, due to the toxic and carcinogenic effects on human health and adverse environmental issues [3]. However HCHs are still found at high concentrations worldwide in areas of former pesticide production, since other HCH-isomers as by-products of Lindane production were dumped at production sites [4]. Plants and crops grown on contaminated land can accumulate HCH [5], which is a potential entry of HCH to food webs. Concentration between 1 and 10 μg g^{-1} dry weight plant biomass has been found in the vicinity contaminated site [2] which is far above the acceptable levels and raises concerns when used as a food stock. However, contaminated biomass after phytoremediation [6,7] might be used for biogas production and opens an option for using polluted land [8]. Therefore, for clean-up, phytoremediation can be used in the contaminated field and the HCH-contaminated biomass can be used as substrate of AD for biogas production.

An understanding on the fate of HCHs in AD is required for the full-scale application. Anaerobic degradation processes metabolize pollutants through reductive pathways with mineralization or

reduction of highly electrophilic halo- and nitro-groups, to less toxic compounds by transferring electrons to the contaminant [9–11]. Particularly reductive dehalogenation is favored under anoxic conditions. Thus, HCH as persistent halogenated organic contaminants can be transformed through reductive dehalogenation under anaerobic condition [12–16] and also in biogas system as it was demonstrated in our recent study [8].

The transformation of HCHs during wastewater treatment in up-flow anaerobic sludge blanket reactor (UASB) had been also reported [17,18]. However, the fate of HCH during continuous large-scale AD with plant biomass feedstock and its effect on reactor performance during biogas production was not yet investigated. According to our previous study with batch reactors [8], HCH addition up to 150 mg/L has no negative influence on final methane yield from main substrate and the transformation rates of γ- and α-HCH were high, which demonstrated that AD appears to be a bioremediation option for HCH contaminated biomass.

For this work, we scaled up the AD process to bio-transform HCH in continuous mode, for characterization of the transformation processes as required before utilizing contaminated biomass in large-scale for biogas production. Therefore, a continuous stirred tank reactor (CSTR) was established to investigate the interaction of HCHs and microbiota in larger scale in semi-continuous feeding mode.

The transformation pathway of HCHs can be identified employing metabolite formation and compound-specific stable isotope analysis (CSIA) [19–22]. Fractionation factors of HCH can then be used for comparison with culture studies for characterisation of the transformation pathway in AD process [23–26]. Moreover, assessment of the main methanogenic pathways in biogas reactors [27–30] can be deduced from isotope composition of the produced methane [31–

36]. In addition, batch experiment with ^{13}C-labelled benzene was conducted for investigation of the complete mineralisation of HCHs to CH_4 and CO_2.

Overall, we evaluated the potential application of AD system for treatment of HCH-contaminated biomass in a technical laboratory-scale CSTR. The specific objectives of this study were to: (i) monitor the convential operation of CSTR with addition of HCH isomers (γ, α and β); (ii) prove the potential application of AD for treatment of HCH-contaminated biomass in continuous reactor mode; (iii) characterize the biotransformation pathways of HCHs and the effect of various isomers on microbiota in AD; (iv) show the potential conversion of HCHs to methane and CO_2 in AD system.

2. Materials and Methods

2.1. Substrate and Inoculum

Maize silage (Total solids (TS) = 25.47%, VS (volatile solids) = 96.51% of TS) was used as substrate. The inoculum (TS = 3.41%, VS = 72.20% TS) was sieved biogas slurry taken from the main reactor of a pilot-scale biogas plant which used maize silage and cattle manure as substrate with an organic loading rate (OLR) of 3.5 $g_{vs}L^{-1}day^{-1}$ and hydraulic retention time (HRT) of 47 days. HCH isomers (γ-, α- and β-HCH, separately, analytical purity of 99%) and hexachlorobenzene (HCB) (Lot 60119, analytical purity of 99%), were obtained from Sigma-Aldrich (Munich, Germany). Final concentration of HCH (each isomer) in the reactors was set as 50 μM based on the literature value [37] and our previous inhibition experiment [8] to reflect some potential real case scenarios.

2.2. Setup of CSTRs

Two laboratory-scale CSTRs were operated over more than one year under mesophilic condition (38-40℃) with maize silage as exclusive substrate. One reactor (reactor R4.36) with HCH addition was set up to investigate the interaction of HCH with microbiota; another reactor (reactor R4.35) was operated as the control experiment without addition of HCH. The total reactor volume was 15 L with 10 L working volume. The whole running period was divided into 4 stages for R4.36 after the start-up: the steady phase for establishing the biogas process (phase I), the addition of γ-HCH (phase II), the addition of α-HCH (phase III) and the addition of β-HCH (phase IV) (details of reactor setup see **section A.1.1., Appendix A**).

2.3. Sampling procedure and operating parameters analysis of CSTR

The biogas was collected in a gas bag which was connected to a gas meter TG 05 (Ritter, Germany), then transferred to an AwiFlex gas analyzer (Awite Bioenergie GmbH, Germany) for gas composition measurement [38]. Biogas samples for isotope analysis were taken from the headspace of CSTRs weekly before daily addition of maize silage. They were collected in triplicates using 10-ml gas-tight vacuumed vials for carbon isotope composition [33].

Effluent liquid was periodically collected from both reactors at the same time: (i) 50 mL liquid were stored in 120 mL serum bottle at -20 ℃ for extraction of HCH and its metabolites, to measure the concentration and carbon isotope composition. The detailed protocol was described in our previous publication [8]. (ii) Another 50 mL were taken weekly and centrifuged at 10,000 × g, 10 ℃ for 10 min and filtered with a mesh sieve of 1 mm. The filtrate was used for analysis of volatile fatty acid (VFA) and total ammonia nitrogen (TAN) (details of analysis on parameters see **section A.1.2., Appendix A**).

2.4. Microbial community structure analysis

Triplicate 0.5 mL samples were taken from both CSTRs periodically and stored at -20 ℃ for molecular biological analysis. Three samplings for each phase with single HCH isomer were conducted (day 129 for steady phase; days 161, 181 and 197 for γ-HCH phase; days 277 and 301 for α-HCH phase; days 330, 352 and 378 for β-HCH phase). The total genomic DNA was extracted with 'NucleoSpin Soil' kit (Macherey-Nagel GmbH & Co. KG, Düren, Germany) according to the manufacturer's protocol using buffer SL2 with enhancer SX.

The 16S rRNA genes were further amplified and sequenced via Illumina$^{@}$ MiSeq. Shannon index and amplicon sequence variant (ASV) counts (α-diversity) were determined using the R package phyloseq [39]. Differences in bacterial community composition (β-diversity) were calculated using Bray–Curtis dissimilarity index based on rarefied (15063 ASV counts per sample) and square-root-transformed ASV abundances, which are demonstrated via nonmetric multi-dimensional scaling (NMDS) plot. Permutational multivariate analysis of variance (PERMANOVA) [40] were calculated by "adonis2" function in "vegan" R package using 10^6 permutations to determine if different environmental variables (i.e., time, HCH addition and reactor phases) were important factors correlated with shifts in ASV abundance. Further, ASVs which could be used to classify the difference of HCH-added and non-added reactors between reactor phases were identified (hereafter, bioindicators). In order to determine bioindicators, the analyzes were conducted with three steps [41]. First, machine learning derived from Random Forest [42] to calculate variable important ASVs via Mean Decrease Gini for reactor phase and other important factors from the NMDS analysis. Second, the potential bioindicators were those ASVs that only present on machine learning of reactor phase deducting the ASVs that both relevant for reactor phase and other important factors. Third, bioindicators were identified from

147 the above selected ASVs removing those were not statistically significant via the LSMEANS test
148 with pair-wise methods adjusted by false discovery rate (FDR) correction [43,44].

149 The diversity of microbial communities from both reactors was also investigated by terminal
150 restriction fragment length polymorphism (T-RFLP) analysis of methyl-coenzyme M reductase
151 alpha-subunit (*mcrA*) genes for archaea and the variable regions V1–V3 of bacterial 16S rRNA
152 gene fragments for bacteria [45–48].

153 **2.5. Batch experiments with labelled benzene-$^{13}C_6$ in AD**

154 For evaluating further degradation of the HCH metabolite benzene, labelled compound (benzene-
155 $^{13}C_6$) with final concentration of 100 µM was spiked with a glass syringe as pure compound into
156 serum bottles filled with 50 ml slurry taken from the benzene-added set of automatic methane
157 potential test system (AMPTS, Bioprocess Control Sweden AB, Sweden) described in our
158 previous study [8]. The preparation was done in an anaerobic glove box (gas atmosphere—N_2:H_2
159 (95:5); Coy Laboratory Products Inc., USA). Control set was prepared simultaneously in
160 triplicate only with slurry from benzene-added set.

161 **2.6. Enantioselectivity and Enantiomer-specific stable isotope fractionation of α-HCH**

162 In order to derive enantioselectivity (ES), 21.8 mg/L (75 µmol/L) of α-HCH were added
163 respectively into 120 mL bottles with 50 mL biogas digestate from CSTR effluent. The
164 headspace was flushed with nitrogen for 5 min before the bottles were closed with Teflon™-
165 coated butyl rubber septa and crimped. Fifteen parallel bottles for each isomer were prepared for
166 sampling at different time points. (details on calculation of ES see **section A.1.5., Appendix A**).
167 In addition, triplicate negative controls with sterilized digestate and α-HCH were conducted. In

the sterilized control concentration remain stable and no metabolites were detected, showing that biotransformation only occurred in active biogas digestate (data not shown).

3. Results

3.1. Performance of CSTRs

3.1.1. Methane production, total ammonium nitrogen and volatile fatty acids for characterization of AD processes

In phase I (steady phase), the average specific methane production (SMP) was 286 ± 32.1 and 283 ± 27.7 mL_N/g VS in the control reactor and the reactor later used for HCH supplementation, respectively, and were statistically identical. After addition of γ-HCH in phase II, SMPs were 287 ± 36.5 and 306 ± 36.7 mL_N/g VS in the control and HCH-added reactor, respectively; in phase III, the SMPs were 311 ± 43.2 and 308 ± 44.2 mL_N/g VS in control and α-HCH reactors, respectively; in phase IV, SMPs of 266 ± 31.8 and 283 ± 39.4 mL_N/g VS were observed in control and β-HCH reactors, respectively (**Fig. 1a and Table 1**). The SMPs were statistically identical in both reactors during phase I to IV, indicating addition of HCHs did not affect the SMP. Methane and CO_2 contents were 54~56% and 43~45%, respectively, during the whole running period (**Fig. 1b**).

In start-up phase, concentrations of VFAs and acetate were 95.1 ± 68.5 and 66.4 ± 45.1 mg/L for control reactor, respectively (108.4 ± 81.2 and 64.8 ± 42.4 mg/L for HCH-added reactor). In phase II and III (γ-HCH and α-HCH phase), the concentrations of VFAs and acetate were generally slightly higher in HCH-added reactor compared to the control reactor (**Fig. 1c** and **Fig. A.2**). In general, there was a significant difference between concentrations of VFAs in these two

189 reactors (p-value= 0.02187, $p < 0.05$; one way ANOVA analysis), nevertheless all these values
190 were still within conventional ranges of stable operation.

191 **3.1.2. Concentration and stable isotope analysis for biotransformation of HCHs**

192 Concentrations and stable isotope compositions of HCHs and the metabolites are shown in **Fig. 2**.
193 In phase II (day 147-187), the addition of HCH was about 50 µM for the whole reactor. Both γ-
194 and α-HCH were nearly completely removed within 14 days and 7 days, respectively. The γ-
195 HCH degraded faster after day 173 with a removal below the limit of detection within 3 days.
196 Similarly, in phase III (day 245-275), α-HCH transformed faster at day 253 compared to addition
197 at day 245. In phase II and III, benzene and MCB were detected as metabolites. No
198 transformation of β-HCH was detected in phase IV of our system from day 330 to day 360,
199 which was deduced from the constant concentration and lack of metabolites.

200 Carbon isotope enrichment of γ-HCH and α-HCH was observed from -27.5 to -21.0‰ and from -
201 27.5 to -24.0‰, respectively (**Fig. 2**). The variations were in a similar order with respect to the
202 isotope enrichment of $\delta^{13}C$ observed in our previous study from-27.5 to -17.0‰ for γ-HCH and
203 from -27.5 to -23.0‰ for α-HCH [8], however the number of data do not allow quantifying the
204 isotope fractionation using the Rayleigh approach in the continuous flow reactor. The $\delta^{13}C$
205 values of β-HCH were stable at ca. -27.5‰ in phase IV. The $\delta^{13}C$ values of chlorobenzene
206 ranged from -24.8 to -18.2‰ in γ-HCH phase and from -28.1 to -25.1‰ in α-HCH phase,
207 showing same increasing tendency as HCH isomers. Whereas $\delta^{13}C$ values of benzene was
208 ranging from -29.8 to -27.2‰ but the isotope measurement of this metabolite was only possible
209 in few samples, due to the low concentrations (**Fig. 2**).

3.1.3. Microbial community structure

NMDS plots for bacterial microbial community structures of all selected samples in both reactors are shown in **Fig. A.5**. In the PERMANOVA main test (**Table A.2**), significant difference (Pseudo-F = 2.25788, P = 0.004693, **Fig. A.5b**) was observed between the two reactors taken the reactor phase as a factor. Although, no significant difference was shown between both reactors taking HCH addition as a factor (Pseudo-F = 1.64138, P = 0.095825, **Fig. A.5b**) we observed statistically significant differences when comparing the different reactor phases to the control samples collected in the same dates (**Fig. A.5.c-e**). In addition, time was also found as important factor between early and late phases with the significant difference (Pseudo-F = 9.07219 and P = 0.000012) (**Fig. A.5a**). For identification of the bioindicators which could differentiate HCH-added reactor and control reactor responding to reactor phase, three steps were conducted. First, as reactor phase and time both were important factors, 35 variable important ASVs were selected for each of them based on random forest analysis (**Fig. A.6** & **A.7**). Moreover, confusion matrices were generated for classification of the samples using the rarefied ASV relative abundances as numeric values with time, HCH-addition and HCH phase as factors (**Table A.1**). Second, 28 ASVs were obtained as potential bioindicators relevant to reactor phase rather than time after machine learning (**Table A.3**). Third, 10 ASVs significantly different ($P < 0.05$) to reactor phase via the LSMEANS test by FDR multiple correction (**Appendix B** & **C**) selected from last two steps, were identified as bioindicators. Boxplots were used for every chosen bioindicator to depict statistically different ($P < 0.05$) contribution of ASVs caused by addition of different HCH isomer in HCH-added reactor and control reactor (**Fig. A.8**). To demonstrate ASVs which were significantly associated with the pairwise reactor phases ($P < 0.05$) (**Fig. 3**), these ASVs were separated into four groups: steady phase vs. β-HCH phase (Group1); γ-HCH

phase vs. α-HCH phase (Group2); γ-HCH phase vs. β-HCH phase (Group3); α-HCH phase vs. β-HCH phase (Group4). Among the 10 ASVs identified as bioindicators, 8 ASVs are classified to order *Clostridiales*, which provide the relations of HCH addition with the abundance of *Clostridiales*. The other 2 ASVs are assigned to order *Hydrogenisporales*.

The variation of methanogens in control reactor and HCH-added reactor at different phases was demonstrated via T-RFLP (**Fig. A.9**). The bacterial and archaeal community compositions in both reactors converged toward different direction in intra-sample variability NMDS plots (**Fig. A.10**). Significant difference was observed in archaea between the control reactor and HCH-added reactor (PERMANOVA main test; pseudo-F = 2.986, P = 0.015, see also **Fig. A.10a**). However, no significant difference was observed in bacteria from the NMDS plots (PERMANOVA main test; pseudo-F = 2.205, P >0.05, see also **Fig. A.10b**). The correlation between the communities and reactor parameters is depicted as arrows in the NMDS plots. The direction and length of arrow which represents the abundance of genus *Methanosaeta* showed strong correlation with HCH addition. Furthermore, concentration of acetate was also correlated with addition of HCH solution (**Fig. A.2a**).

Taking both results from MiSeq and T-RFLP into consideration, HCH-added reactor had a higher abundance of *Methanosaeta* and *Clostridiales* compared to the control reactor. The isotope signature of methane indicates an increase in acetoclastic methanogens, correlating with the increased *Methanosaeta*.

3.2. Labelled benzene-$^{13}C_6$ degradation in AD system

The further degradation and mineralization of benzene was observed in the microcosms prepared with slurry from a benzene supplemented batch system of our previous study and amended with

255 $^{13}C_6$-labelled benzene. Significant amounts of ^{13}C labelled CO_2 ($\delta^{13}C$ = +299.0 ± 0.2‰) and

256 methane ($\delta^{13}C$ = 87.3 ± 0.4‰) were detected after 116 days (**Fig. 4**), which is a direct evidence

257 for the conversion of labelled benzene $^{13}C_6$ to CO_2 and methane. Meanwhile, in control set the

258 carbon stable isotope composition of methane and CO_2 remained stable at -48.8 ± 1.3 ‰ and

259 14.4 ± 0.3 ‰, respectively.

260 The slurry from benzene-added set of AMPTS was also sequenced via Illumina@ MiSeq.

261 Microbes, such as class *Spirochaetes*, class *Epsilonproteobacteria*, order *Thermotogales*, family

262 *Peptococcaceae*, genera *Pelotomaculum* and *Desulfosporosinus*, potentially associated with

263 benzene degradation [49–53] were found in benzene amended slurry from our system (see

264 **Appendix D** & **E**).

265 **3.3.Enantiomer fractionation (EF) and enantiomer-specific isotope fractionation of α-HCH**

266 **in batch experiment**

267 In the sterilized control experiment, $\delta^{13}C$ values of (-) and (+) α-HCH were stable at -31.9 ± 0.5

268 and -30.7 ± 0.2‰, respectively; the concentration remained constant at ca. 75 µmol/L, showing

269 that no abiotic transformation took place. In active biogas slurry, $\delta^{13}C$ values of (-) and (+) α-

270 HCH were both enriched, ranging from -32.1 ± 0.4 to -29.3 ± 0.4‰ and from -30.7 ± 0.1 to -26.9

271 ± 0.1‰, respectively **(Fig. 5a**). According to Rayleigh equation, carbon isotope fractionation

272 factors (ε_c) of (+) and (-) *α*-HCH are -4.1 ± 0.3‰ and -4.6 ± 0.4‰, respectively (**Fig. 5c**).

273 Simultaneously, EF of (-) α-HCH increased from 0.50 to 0.56. The degradation kinetics of (-) α-

274 HCH and (+) α-HCH in biogas slurry with values of 0.015 ± 0.001 and 0.020 ± 0.001are shown

275 in **Fig. 5b**, suggesting preferential transformation of (+) α-HCH in AD system. Similar trend was

276 also observed in CSTR and the EF of (-) α-HCH was shifted to 0.57 (**Fig. A.11**). The

277 enantiomeric fractionation was consistent with the enantioselectivity observed in the batch
278 experiment. Thus, (+) α-HCH was preferentially transformed in AD system and can be used as
279 an indicator for biodegradation.

280 **4. Discussion**

281 **4.1. Effect of HCHs on the performance of CSTR**

282 The typical concentration of HCH in plants near the HCH dumpsite was found up to 29 $\mu g \cdot g^{-1}$[2].
283 Concentrations amended in CSTR (50 μM, equal to 243 $\mu g \cdot g^{-1}$) was higher; however, no
284 significant differences in both SBP and SMP were observed between two reactors in all phases
285 with $P > 0.05$. Control and HCH-added reactor had similar pH, TAN concentrations, as well as
286 the content of methane and CO_2; however, relatively higher concentrations of VFAs were
287 detected in the HCH-added reactor, which might be attributed to the addition of HCH. Overall,
288 the conventional parameters in CSTRs had no significant fluctuation caused by HCH-addition at
289 concentration of 50 μM, indicating the potential for treatment of HCH contaminated biomass in
290 AD system under continuous mode. The quality of the maize silage used as the main substrate
291 for feeding was not constant; therefore, it had also influence on the gas production values, but it
292 affected both reactors in a similar way.

293 **4.2. Bioindicators responding to HCH addition in the microbial communities of CSTR**

294 **4.2.1. Dynamics of the bacterial community**

295 Reductive dehalogenation has been proven as main pathway of HCHs transformation in AD
296 system [8], suggesting HCHs as electron acceptors can be co-metabolized by microorganisms.
297 Despite the similar process parameters in the experimental and control reactors, addition of
298 respective HCH isomers in different reactor phases had a significant effect on the microbial

community structures. The communities were classified with confidence up to Genus level due to the size of the amplicon in this study; however, groups belonging to the same taxonomic/phylogenetic group have similar functions. ASVs belonging to order *Clostridiales* were identified as bioindicator responding to HCH-addition, due to the significant variation on abundance. Moreover, ASVs belonging to the class *Dehalococcoidia*, a taxon containing organohalide respiring bacteria [9,54,55], were also found in our system already in the initial phase (see **Appendix D** & **E**). This highlights the intrinsic potential of the AD microbiota to deal with halogenated compounds. Acetogenic bacteria and *Clostridium* sp. were found to be linked to reductive dehalogenation of HCHs in other studies [56,57]. Reductive dechlorination of Lindane was also detected from cell-free extracts *of Clostridium rectum* [58] and *Clostridium sphenoides* [59].

4.2.2. Dynamics of the methanogenic community

The dominant methanogens were affiliated to genus *Methanoculleus* in both reactors (**Fig. A.9**). Species affiliated to *Methanoculleus* were dominant methanogens in many biogas-producing reactor systems fed with maize silage and manure [60]. Although this hydrogenotrophic methanogen was predominant in both reactors, the abundance in HCH-added reactor was lower than in control reactor. These small coccoid methanogens are sensitive to detergents, physical and osmotic stresses [61], which might explain the reduced relative abundance of *Methanoculleus* in the experimental reactor after HCHs solution was added.

A significant increase of the abundance of genus *Methanosaeta* in the HCH-added reactor was detected, and it is consistent with the bioindicators derived from Miseq analysis and NMDS plots. The enriched $\delta^{13}C\text{-}CH_4$ caused by β-HCH addition also confirmed the increased abundance of putative acetotrophic methanogens (**Fig. A.9**). It was reported that *Methanosaeta* spp.

outcompeted *Methanosarcina* spp.as acetotrophic methanogens when acetate concentrations were lower than 200 mg L^{-1} [62], similar to observations in this study. *Methanosaeta* and *Methanosarcina* spp. were dominant methanogens in anaerobic reactors treating wastewater with other halogenated compounds such as tetrachloroethylene and 2-chlorophenol [63,64]. Genus *Methanosaeta* comprises anaerobic, nonmotile, non-sporeforming rods with flat ends in morphology and it can form flexible filaments in a continuous, tubular, proteinaceous sheath for resisting harmful chemical agents [65]. Thus, it was assumed that its cell envelope structure was conducive to resist the toxicity of HCHs, which resulted in increased predominance of *Methanosaeta* in HCH-added reactor.

4.3. Biodegradation of HCH to biogas

4.3.1. Biotransformation of HCH to benzene and chlorobenzene in AD

In this study, we proved the biotransformation of HCH not only from the decrease in concentration and the detection of metabolites, but also from the stable isotope compositions of HCH and metabolites, which provides a new unambiguous analysis method for biotransformation of chemicals in AD system. In conventional studies, the indication on biodegradation of chemicals was deduced from the reduced concentration during the reaction period, which is a controversial issue since absorption and volatilization of chemicals in AD slurry can also lead to the decrease of concentration. Biotransformation of HCH can be confirmed from the reduced concentration and enriched carbon isotope composition of HCH during γ and α-HCH reactor phase, as well as from detection of metabolites and the enrichment of carbon isotope composition of chlorobenzene.

4.3.2. Mineralization of labelled benzene-$^{13}C_6$ to biogas

The formation of labelled methane and CO_2 from benzene proved that the detected HCH metabolites benzene can be further degraded. The benzene mineralization to CO_2 and methane under methanogenic conditions was reported [51,66–68], however were not detected in AD systems before. The putative pathway of benzene is proposed starting with the conversion of benzene to phenol by hydroxylation or to toluene by methylation [69] and subsequent transformation to benzoate [70]. Further degradation can be achieved via benzoyl-CoA pathway [71].

The conversion of total amount of benzene to CH_4 was estimated, to evaluate the contribution of benzene degradation to enhancement on methane yield. If there is 100% conversion of 100 µmol benzene, ca. 9.2 mL methane will be produced. The calculation was based on the equation below [72], which is calculated with CO_2 as electron acceptor under methanogenic conditions:

$$4C_6H_6 + 27H_2O \rightarrow 15CH_4 + 9HCO_3^- + 9H^+ \ldots\ldots \quad \textbf{(Eq. 2)}$$

In case of current biomass conversion AD systems, a long storage of digestate is required by the authorities to avoid the residual methane production and its negative climate effect. The retention time in such digestate storage facilities usually exceed 100 days, which would provide the time needed to completely degrade the remaining metabolites benzene to biogas.

To evaluate the interaction of AD and HCHs, the proposed linked pathways during full degradation of α and γ HCH in biogas-producing system is summarized in **Scheme 1**. AD provided the reductive condition for dehalogenation of HCH with H_2 or acetate, produced during fermentation, as electronic donor. Furthermore, the metabolite benzene was mineralized to biogas in AD. HCH with concentration higher than 150 mg/L can cause temporary inhibition on

365 acetoclastic methanogenesis [8]. In CSTR setup, HCH contaminated plants showed no negative
366 influence on methane production. In general, α and γ HCH can be degraded to methane and CO_2
367 in AD systems, indicating the positive potential of HCH-contaminated biomass for biogas
368 production not only from plant substrate but also from the contaminant HCH.

369 **4.4.Structure selectivity of HCHs in anaerobic digestion**

370 **4.4.1. Diastereoselectivity of HCHs**

371 The isomers of HCHs denoted by Greek letters (α, β, γ, δ, ε, η, and θ, see **section A.1**, **Appendix**
372 **A**) differ in their axial- equatorial substitution pattern around the ring [73]. In our previous study,
373 it was assumed that transformation mechanism of HCHs in AD system was reductive
374 dehalogenation [8]. In this study, α, β and γ isomers were tested in CSTR system, among which,
375 γ isomer possessing three axial Cl atoms transformed faster than the α isomer with two axial Cl
376 atoms. Subsequently, no transformation of β isomer without axial Cl atom was observed in AD
377 system. Thus, it was assumed that dihaloelimination or anti-periplanar dehydrochlorination
378 occurs to eliminate sequentially chlorine resulting in the final metabolites as chlorobenzene and
379 benzene [8,15,74]. The transformed order of HCH isomers in our study is consistent with the
380 report of Buser *et al* [74]. The results suggest that the transformation rate of HCH in AD system
381 was associated with the number of axial Cl, since axial atoms are easier to be cleaved from the
382 parent compound than equatorial Cl atoms.

383 **4.4.2. Enantioselectivity of α-HCH**

384 Enantioselectivity for α-HCH in biogas reactor is significantly different from the aerobic
385 degradation in research by Bashir *et al* [25]. Variation of (EF) (−), from 0.45 to 0.14 in
386 *Sphingobium indicum* strain B90A and 0.50 to 0.24 for *Sphingobium indicum* strain UT26, was

discovered, indicating that (-) α-HCH was preferentially degraded in oxic condition [25]. Contrarily, EF (-) changed from 0.50 to 0.56, which was associated with slight preference towards the transformation of (+) α-HCH in our AD system. The ES values of 0.14 is different from the aerobic transformation by *Sphingobium indicum* strain B90A with ES of -0.45 [21]. However, no enantioselectivity of α-HCH during the reductive dehalogenation by the *Dehalococcoides mccartyi* strains in anoxic condition was observed [22]. In contrast, the enantio-selectivity in this study is consistent as reported by Buser and Müller with the faster degradation of (+) α-HCH compared to (-)α-HCH in sewage sludge [74].

5. Conclusion and outlook

The addition of HCHs in CSTR showed no negative influence on conventional reactor parameters and methanogenesis at the concentration range found in biomass grown on contaminated areas. The robust microbiota of AD process can adapt to the toxic HCH isomers and even successful biodegrade γ and α isomers. In addition, benzene can be degraded to methane and CO_2, deduced from the isotope labelling test, indicating the potential full conversion of HCHs to biogas with long retention time of post digestion. The isotope and enantiomer fractionation can be used to characterize the transformation in AD systems. The isotope fractionation pattern of HCH might be used to evaluate the process and the isotope fractionation pattern of CH_4 and CO_2 to monitor the status of the AD reactor. In summary, phytoremediation coupled to AD and subsequent fertilization using digestate is a promising strategy for economic use and simultaneous remediation of POPs contaminated lands.

Conflicts of interest

There are no conflicts to declare.

Acknowledgements

Shujuan Lian was funded by the China Scholarship Council [File No. 201404910520] and supported by the Helmholtz Interdisciplinary Graduate School for Environmental Research. The experimental setup of AMPTS and CSTR was supported by DBFZ (German Biomass Research Centre). We acknowledge the financial support from the German-Israeli Foundation for Research and Development (GIF) Grant no. I-1368-307.8/2016 ("Prediction of chiral and isotope enrichment during the transformations of halo-organic pollutants: Mechanistic and QSAR approaches"). Thanks to Ute Lohse for supplying help with microbial analysis. Thanks to Steffen Kümmel for helping with isotope measurements and to Monika Möder for freeze-drying samples. And thanks to Rodolfo Brizola Toscan for helping with data process of MiSeq. Dr. Ulisses Nunes da Rocha and Dr. Joao Pedro Saraiva are financed by the Helmholtz Association VH-NG-1248 Micro 'Big Data'. The study was supported by the Initiative and Networking Fund of the Helmholtz Association.

Appendix A. Supplementary material

Supplementary material associated with this article can be found, in the online version.

Appendix B. Supplementary Table A.4

Supplementary Table A.4 associated with this article can be found, in the online version.

Appendix C. Supplementary Table A.5

Supplementary Table A.5 associated with this article can be found, in the online version.

Appendix D. Supplementary Table A.6

Supplementary Table A.6 associated with this article can be found, in the online version.

Appendix E. Supplementary Table A.7

Supplementary Table A.7 associated with this article can be found, in the online version.

Appendix F. Xiao Liu et al., 2019; manuscript in review, for review only

Appendix G. Yaqing Liu et al., 2019; manuscript in review, for review only

Figure captions

Fig. 1 Methane yield (a), methane content (b) and total VFAs (c) in CSTRs over phases I to IV. Data were corrected to pressure (101.325 kPa) and standard temperature (273.15 k), thus are reported as normalized milliliters (mLN) per gram of volatile solid (VS).

Fig. 2 Concentrations and carbon isotope compositions of γ-HCH (a&b), α-HCH (c&d), β-HCH (e&f) and metabolites (chlorobenzene and benzene). Values of 0 indicate that they were below the detection limit. Black arrows mean adjustment of the concentration to 50 μM and blue arrows represent the addition of HCH to 12 μM. Values of $\delta^{13}C$ are associated with concentration and the data below the confidential interval of detection via GC-IRMS are not shown here.

Fig. 3 Relative abundance distribution of ASVs used as bioindicators in the control CSTR and HCH-added CSTR per sample.

ASVs separated in 4 different groups depending on statistic differences ($P < 0.05$) of abundance using the LSMEANS test with FDR multiple correction, based on the interaction of pairwise reactor phases: steady phase vs. β-HCH phase (Group1); γ-HCH phase vs. α-HCH phase (Group2); γ-HCH phase vs. β-HCH phase (Group3); α-HCH phase vs. β-HCH phase (Group4).

Fig. 4 Carbon isotope signatures of methane (a) and CO_2 (b) in batch experiment with addition of benzene-$^{13}C_6$.

Fig. 5 Enantiomer fractionation (EF) of (-) α-HCH and carbon isotope compositions of (-) / (+) α-HCH in biogas slurry (batch experiment) (a); the degradation kinetics of (-) α-HCH (◆) and (+) α-HCH (■) in biogas slurry (b); carbon stable isotope enrichment factors of (-) / (+) α-HCH (c).

References

[1] X. Liu, L. Wu, S. Kümmel, H. Richnow, Characterizing the biotransformation of hexachlorocyclohexane in wheat using compound-specific stable isotope analysis and enantiomer fraction analysis, (2019) submitted, see Appendix F, manuscript in review.

[2] L. Wu, Y. Liu, X. Liu, A. Bajaj, M. Sharma, R. Lal, H. Richnow, Isotope fractionation approach to characterize the reactive transport processes governing the fate of hexachlorocyclohexanes at a contaminated site in India, Environ. Int. 132 (2019) 105036.

[3] J. Vijgen, P.C. Abhilash, Y.F. Li, R. Lal, M. Forter, J. Torres, N. Singh, M. Yunus, C. Tian, A. Schäffer, R. Weber, Hexachlorocyclohexane (HCH) as new Stockholm Convention POPs-a global perspective on the management of Lindane and its waste isomers, Environ. Sci. Pollut. Res. 18 (2011) 152–162.

[4] W. Slooff, A. Matthijsen, J. Canton, H. Eerens, C. van Gestel, E. Heijna-Merkus, P. Greve, P. Janssen, J. van Koten-Vermeulen, J. Knoop, Integrated criteria document hexachlorocyclohexanes, 1988.

[5] L. Wu, S. Moses, Y. Liu, J. Renpenning, H.H. Richnow, A concept for studying the transformation reaction of hexachlorocyclohexanes in food webs using multi-element compound-specific isotope analysis, Anal. Chim. Acta. 1064 (2019) 56–64.

[6] S. Hussain, T. Siddique, M. Arshad, M. Saleem, Bioremediation and phytoremediation of pesticides: recent advances, Crit. Rev. Environ. Sci. Technol. 39 (2009) 843–907.

[7] N. Agrawal, S.K. Shahi, An environmental cleanup strategy - microbial transformation of xenobiotic compounds, Int. J. Curr. Microbiol. Appl. Sci. 4 (2015) 429–461.

[8] S. Lian, M. Nikolausz, I. Nijenhuis, A.F. Leite, H.H. Richnow, Biotransformation and inhibition effects of hexachlorocyclohexanes during biogas production from contaminated biomass characterized by isotope fractionation concepts, Bioresour. Technol. 250 (2018) 683–690.

[9] T. Kaufhold, M. Schmidt, D. Cichocka, M. Nikolausz, I. Nijenhuis, Dehalogenation of diverse halogenated substrates by a highly enriched *Dehalococcoides*-containing culture derived from the contaminated mega-site in Bitterfeld, FEMS Microbiol. Ecol. 83 (2013) 176–188.

[10] J. Ye, A. Singh, O.P. Ward, Biodegradation of nitroaromatics and other nitrogen-containing xenobiotics, World J. Microbiol. Biotechnol. 20 (2004) 117–135.

[11] K.J. Rockne, K.R. Reddy, W.T. Street, Bioremediation of contaminated sites, in: Int. e-Conference Mod. Trends Found. Eng. Geotech. Challenges Solut., 2003: pp. 1–22.

[12] I. V. Robles-González, E. Ríos-Leal, I. Sastre-Conde, F. Fava, N. Rinderknecht-Seijas, H.M. Poggi-Varaldo, Slurry bioreactors with simultaneous electron acceptors for bioremediation of an agricultural soil polluted with Lindane, Process Biochem. 47 (2012) 1640–1648.

[13] S. Bashir, K.L. Hitzfeld, M. Gehre, H.H. Richnow, A. Fischer, Evaluating degradation of hexachlorcyclohexane (HCH) isomers within a contaminated aquifer using compound-specific stable carbon isotope analysis (CSIA), Water Res. 71 (2015) 187–196.

[14] P.J.M. Middeldorp, M. Jaspers, A.J.B. Zehnder, G. Schraa, Biotransformation of α-, β-, γ-, and δ -hexachlorocyclohexane under methanogenic conditions, Environ. Sci. Technol. 30

(1996) 2345–2349.

[15] R. Lal, G. Pandey, P. Sharma, K. Kumari, S. Malhotra, R. Pandey, V. Raina, H.E. Kohler, C. Holliger, C. Jackson, J.G. Oakeshott, Biochemistry of microbial degradation of hexachlorocyclohexane and prospects for bioremediation, Microbiol. Mol. Biol. Rev. 74 (2010) 58–80.

[16] P.J.M. Middeldorp, W. Van Doesburg, G. Schraa, A.J.M. Stams, Reductive dechlorination of hexachlorocyclohexane (HCH) isomers in soil under anaerobic conditions, Biodegradation. 16 (2005) 283–290.

[17] T.P. Baczynski, J. Kurbiel, Identification of operational parameters critical for removal of selected chlorinated pesticides in UASB reactor, Proc. 9th World Congr. Anaerob. Dig. Anaerob. Convers. Sustain. 1 (2001).

[18] P. Bhatt, M.S. Kumar, S.N. Mudliar, T. Chakrabarti, Biodegradation of tech-hexachlorocyclohexane in a upflow anaerobic sludge blanket (UASB) reactor, Bioresour. Technol. 97 (2006) 824–830.

[19] C. Wiegert, Application of two dimensional compound specific carbon-chlorine isotope analyses for degradation monitoring and assessment of organic pollutants in contaminated soil and groundwater, Dr. Thesis, Stock. Univ. (2013).

[20] S.A. Law, T.F. Bidleman, M.J. Martin, Evidence of enantioselective degradation of α-hexachlorocyclohexane in groundwater, Env. Sci Technol. 38 (2004) 1633–1638.

[21] Y. Liu, L. Wu, P. Kohli, R. Kumar, H. Stryhanyuk, I. Nijenhuis, R. Lal, H.-H. Richnow, Enantiomer and carbon isotope fractionation of α-hexachlorocyclohexane by *Sphingobium*

indicum strain B90A and the corresponding enzymes, Environ. Sci. Technol. 53 (2019) 8715-8724.

[22] Y. Liu, J. Liu, J. Renpenning, I. Nijenhuis, H.-H. Richnow, Dual C-Cl isotope analysis for characterizing the reductive dechlorination of α- and γ-hexachlorocyclohexane by two *Dehalococcoides mccartyi* strains and an Enrichment culture, (2019) submitted, see Appendix G, manuscript in review.

[23] S.L. Badea, C. Vogt, S. Weber, A.F. Danet, H.H. Richnow, Stable isotope fractionation of γ-hexachlorocyclohexane (Lindane) during reductive dechlorination by two strains of sulfate-reducing bacteria, Environ. Sci. Technol. 43 (2009) 3155–3161.

[24] S.L. Badea, C. Vogt, M. Gehre, A. Fischer, A.F. Danet, H.H. Richnow, Development of an enantiomer-specific stable carbon isotope analysis (ESIA) method for assessing the fate of α-hexachlorocyclohexane in the environment, Rapid Commun. Mass Spectrom. 25 (2011) 1363–1372.

[25] S. Bashir, A. Fischer, I. Nijenhuis, H.H. Richnow, Enantioselective carbon stable isotope fractionation of hexachlorocyclohexane during aerobic biodegradation by *Sphingobium* spp., Environ. Sci. Technol. 47 (2013) 11432–11439.

[26] S. Bashir, Assessment of in situ transformation of Hexachlorocyclohexane using carbon stable isotope analysis (CSIA) (Doctoral dissertation), Eberhard Karls Universität Tübingen, 2014.

[27] D. Polag, L.C. Krapf, H. Heuwinkel, S. Laukenmann, J. Lelieveld, F. Keppler, Stable carbon isotopes of methane for real-time process monitoring in anaerobic digesters, Eng.

Life Sci. 14 (2014) 153–160.

[28] D. Polag, T. May, L. Müller, H. König, F. Jacobi, S. Laukenmann, F. Keppler, Online monitoring of stable carbon isotopes of methane in anaerobic digestion as a new tool for early warning of process instability, Bioresour. Technol. 197 (2015) 161–170.

[29] Z. Lv, M. Hu, H. Harms, H.H. Richnow, J. Liebetrau, M. Nikolausz, H. Hermann, J. Liebetrau, M. Nikolausz, Stable isotope composition of biogas allows early warning of complete process failure as a result of ammonia inhibition in anaerobic digesters, Bioresour. Technol. 167 (2014) 251–259.

[30] J. De Vrieze, M. De Waele, P. Boeckx, N. Boon, Isotope fractionation in biogas allows direct microbial community stability monitoring in anaerobic digestion, Environ. Sci. Technol. 52 (2018) 6704–6713.

[31] J.A. Krzycki, W.R. Kenealy, M.J. Deniro, J.G. Zeikusl, Stable carbon isotope fractionation by *Methanosarcina barkeri* during methanogenesis from acetate, methanol, or carbon dioxide-hydrogen, Appl. Environ. Microbiol. 53 (1987) 2597–2599.

[32] R. Conrad, Quantification of methanogenic pathways using stable carbon isotopic signatures: A review and a proposal, Org. Geochem. 36 (2005) 739–752.

[33] S. Laukenmann, D. Polag, M. Greule, A. Gronauer, Identification of methanogenic pathways in anaerobic digesters using stable carbon isotopes, Eng. Life Sci. 10 (2010) 509–514.

[34] P.E. Galand, K. Yrjälä, R. Conrad, Stable carbon isotope fractionation during methanogenesis in three boreal peatland ecosystems, Biogeosciences. 7 (2010) 3893–3900.

562 [35] H. Penning, P. Claus, P. Casper, R. Conrad, Carbon isotope fractionation during
563 acetoclastic methanogenesis by *Methanosaeta concilii* in culture and a lake sediment,
564 Appl. Environ. Microbiol. 72 (2006) 5648–5652.

565 [36] E.R.C. Hornibrook, F.J. Longstaffe, W.S. Fyfe, Evolution of stable carbon isotope
566 compositions for methane and carbon dioxide in freshwater wetlands and other anaerobic
567 environments, Geochim. Cosmochim. Acta. 64 (2000) 1013–1027.

568 [37] J.C. Quintero, M.T. Moreira, J.M. Lema, G. Feijoo, An anaerobic bioreactor allows the
569 efficient degradation of HCH isomers in soil slurry, Chemosphere. 63 (2006) 1005–1013.

570 [38] D.G. Mulat, H.F. Jacobi, A. Feilberg, A.P.S. Adamsen, H.-H. Richnow, M. Nikolausz,
571 Changing feeding regimes to demonstrate flexible biogas production: effects on process
572 performance, microbial community structure, and methanogenesis pathways, Appl.
573 Environ. Microbiol. 82 (2016) 438–449.

574 [39] P.J. McMurdie, S. Holmes, phyloseq: an R package for reproducible interactive analysis
575 and graphics of microbiome census data, PLoS One. 8 (2013) 1–11.

576 [40] M.J. Anderson, Permutational multivariate analysis of variance (PERMANOVA), Wiley
577 StatsRef Stat. Ref. Online. (2017) 1–15.

578 [41] P.M. Rosado, D.C.A. Leite, G.A.S. Duarte, R.M. Chaloub, G. Jospin, U. Nunes da Rocha,
579 J. P. Saraiva, F. Dini-Andreote, J.A. Eisen, D.G. Bourne, R.S. Peixoto, Marine probiotics:
580 increasing coral resistance to bleaching through microbiome manipulation, ISME J. (2018)
581 Published: 05 December 2018.

582 [42] A. Liaw, M. Wiener, Classification and regression by randomForest, R News. 2/3 (2002)

583 18–22.

584 [43] A. V. Longo, K.R. Zamudio, Environmental fluctuations and host skin bacteria shift
585 survival advantage between frogs and their fungal pathogen, ISME J. 11 (2017) 349–361.

586 [44] R. V. Lenth, Least-squares means: the R package lsmeans, J. Stat. Softw. 69 (2016) 1–33.

587 [45] T. Lueders, K.J. Chin, R. Conrad, M. Friedrich, Molecular analyses of methyl-coenzyme
588 M reductase α-subunit (*mcrA*) genes in rice field soil and enrichment cultures reveal the
589 methanogenic phenotype of a novel archaeal lineage, Environ. Microbiol. 3 (2001) 194–
590 204.

591 [46] J.D. Neufeld, W.W. Mohn, V. De Lorenzo, Composition of microbial communities in
592 hexachlorocyclohexane (HCH) contaminated soils from Spain revealed with a habitat-
593 specific microarray, Environ. Microbiol. 8 (2006) 126–140.

594 [47] N. Sangwan, P. Lata, V. Dwivedi, A. Singh, N. Niharika, J. Kaur, S. Anand, J. Malhotra,
595 S. Jindal, A. Nigam, D. Lal, A. Dua, A. Saxena, N. Garg, M. Verma, J. Kaur, U.
596 Mukherjee, J.A. Gilbert, S.E. Dowd, R. Raman, P. Khurana, J.P. Khurana, R. Lal,
597 Comparative metagenomic analysis of soil microbial communities across three
598 hexachlorocyclohexane contamination levels, PLoS One. 7 (2012) 1–12.

599 [48] M.J. Whiticar, E. Faber, M. Schoell, Biogenic methane formation in marine and
600 freshwater environments: CO_2 reduction vs acetate fermentation - isotope evidence,
601 Geochim. Cosmochim. Acta. 50 (1986) 693–709.

602 [49] M. Nales, B.J. Butler, E.A. Edwards, Anaerobic benzene biodegradation: a microcosm
603 survey, Bioremediat. J. 2 (1998) 125–144.

[50] J.N. Rooney-varga, R.T. Anderson, J.L. Fraga, D.R. Lovley, Microbial communities associated with anaerobic benzene degradation in a petroleum-contaminated aquifer, Appl. Environ. Microbiol. 65 (1999) 3056–3063.

[51] C. Vogt, S. Kleinsteuber, H.H. Richnow, Anaerobic benzene degradation by bacteria, Microb. Biotechnol. 4 (2011) 710–724.

[52] S. Atashgahi, B. Hornung, M.J. van der Waals, U. Nunes da Rocha, F. Hugenholtz, B. Nijsse, D. Molenaar, R. van Spanning, A.J.M. Stams, J. Gerritse, H. Smidt, A benzene-degrading nitrate-reducing microbial consortium displays aerobic and anaerobic benzene degradation pathways, Sci. Rep. (2018) 1–12.

[53] M.J. van der Waals, C. Pijls, A.J.C. Sinke, A.A.M. Langenhoff, H. Smidt, J. Gerritse, Anaerobic degradation of a mixture of MtBE, EtBE, TBA, and benzene under different redox conditions, Appl. Microbiol. Biotechnol. 102 (2018) 3387–3397.

[54] B. Matturro, C. Ubaldi, S. Rossetti, Microbiome dynamics of a polychlorobiphenyl (PCB) historically contaminated marine sediment under conditions promoting reductive dechlorination, Front. Microbiol. 7 (2016) 1–14.

[55] S. Bashir, K. Kuntze, C. Vogt, I. Nijenhuis, Anaerobic biotransformation of hexachlorocyclohexane isomers by *Dehalococcoides* species and an enrichment culture, Biodegradation. 29 (2018) 409–418.

[56] B. Camacho-Pérez, E. Ríos-Leal, N. Rinderknecht-Seijas, H.M. Poggi-Varaldo, Enzymes involved in the biodegradation of hexachlorocyclohexane: a mini review, J. Environ. Manage. 95 (2012) S306–S318.

[57] C. Holliger, G. Schraa, Physiological meaning and potential for application of reductive dechlorination by anaerobic bacteria, FEMS Microbiol. Rev. 15 (1994) 297–305.

[58] N. Ohisa, M. Yamaguchil, N. Kurihara, Lindane degradation by cell-free extracts of Clostridium rectum, Arch. Microbiol. 225 (1980) 221–225.

[59] A.D. Heritage, I.C. Macrae, Degradation of Lindane by cell-free preparations of *Clostridium sphenoides*, Appl. Environ. Microbiol. 34 (1977) 222–224.

[60] I. Maus, D. Wibberg, R. Stantscheff, F.G. Eikmeyer, A. Seffner, J. Boelter, R. Szczepanowski, J. Blom, S. Jaenicke, H. König, A. Pühler, A. Schlüter, Complete genome sequence of the hydrogenotrophic, methanogenic archaeon *Methanoculleus bourgensis* strain MS2T, isolated from a sewage sludge digester, J. Bacteriol. 194 (2012) 5487–5488.

[61] G.M. Maestrojuán, D.R. Boone, L. Xun, R.A. Mah, L. Zhang, Transfer of *Methanogenium bourgens*e, *Methanogenium marisnigri*, *Methanogenium olentangyi*, and *Methanogenium thermophilicum* to the genus *Methanoculleus* gen. nov., emendation of *Methanoculleus marisnigri* and *Methanogenium*, and description of new strains of *Methanoculleus bourgense* and *Methanoculleus marisnigri*., Int. J. Syst. Bacteriol. 40 (2009) 117–122.

[62] D. Zheng, L. Raskin, Quantification of *Methanosaeta* species in anaerobic bioreactors using genus- and species-specific hybridization probes, Microb. Ecol. 39 (2000) 246–262.

[63] S.M. Prakash, S.K. Gupta, Biodegradation of tetrachloroethylene in upflow anaerobic sludge blanket reactor, Bioresour. Technol. 72 (2000) 47–54.

[64] L. Beristain-Montiel, S. Martínez-Hernández, F. de M. Cuervo-López, F. Ramírez-Vives, Dynamics of a microbial community exposed to several concentrations of 2-chlorophenol

in an anaerobic sequencing batch reactor, Environ. Technol. 36 (2015) 1776–1784.

[65] Girishchandra B. Patel, G.D. Sprott, *Methanosaeta concilii* gen. nov., sp. nov. ("*Methanothrix concilii*") and *Methanosaeta thermoacetophila* nom, rev., comb. nov., Int. J. Syst. Bacteriol. 40 (1990) 79–82.

[66] J. Kazumi, M.E. Caldwell, J.M. Suflita, D.R. Lovley, L.Y. Young, Anaerobic degradation of benzene in diverse anoxic environments, Environ. Sci. Technol. 31 (1997) 813–818.

[67] X. Liang, C.E. Devine, J. Nelson, B. Sherwood Lollar, S. Zinder, E.A. Edwards, Anaerobic conversion of chlorobenzene and benzene to CH_4 and CO_2 in bioaugmented microcosms, Environ. Sci. Technol. 47 (2013) 2378–2385.

[68] M. Schmidt, D. Wolfram, J. Birkigt, J. Ahlheim, H. Paschke, H.H. Richnow, I. Nijenhuis, Iron oxides stimulate microbial monochlorobenzene in situ transformation in constructed wetlands and laboratory systems, Sci. Total Environ. 472 (2014) 185–193.

[69] S.A. Mancini, C.E. Devine, M. Elsner, M.E. Nandi, A.C. Ulrich, E.A. Edwards, B.S. Lollar, Isotopic evidence suggests different initial reaction mechanisms for anaerobic benzene biodegradation, Environ. Sci. Technol. 42 (2008) 8290–8296.

[70] M.E. Caldwell, J.M. Suflita, Detection of phenol and benzoate as intermediates of anaerobic benzene biodegradation under different terminal electron-accepting conditions, Environ. Sci. Technol. 34 (2000) 1216–1220.

[71] C.S. Harwood, G. Burchhardt, H. Herrmann, G. Fuchs, Anaerobic metabolism of aromatic compounds via the benzoyl-CoA pathway, FEMS Microbiol. Rev. 22 (1998) 439–458.

[72] J.M. Weiner, D.R. Lovley, Rapid benzene degradation in methanogenic sediments from a

667 petroleum-contaminated aquifer, Appl. Environ. Microbiol. 64 (1998) 1937–1939.

668 [73] K.L. Willett, E.M. Ulrich, R.A. Hites, Differential toxicity and environmental fates of
669 hexachlorocyclohexane isomers, Environ. Sci. Technol. 32 (1998) 2197–2207.

670 [74] H.R. Buser, M.D. Müller, Isomer and enantioselective degradation of
671 hexachlorocyclohexane isomers in sewage sludge under anaerobic conditions, Environ.
672 Sci. Technol. 29 (1995) 664–672.

673

Phase	Reactor	HCH addition	SBP (mL_N/g VS)	SMP (mL_N/g VS)	Methane (%)	CO_2 (%)	pH	TAN (NH^{4+}-N/L)	VFAs (mg/L)	Acetate (mg/L)	$\delta^{13}C$-CH_4 (‰)	$\delta^{13}C$-CO_2 (‰)
Phase I (day 90-150)	R4.35	no	511 ± 57.7	286 ± 32.1	55.9 ± 2.1	43.7 ± 2.2	7.41 ± 0.09	1.90 ± 0.17	95.14 ± 68.54	66.38 ± 45.07	-35.7 ± 1.2	11.7 ± 0.5
	R4.36	no	505 ± 51.2	283 ± 27.7	55.9 ± 1.9	43.8 ± 2.0	7.41 ± 0.08	1.90 ± 0.17	108.37 ± 81.21	64.84 ± 42.42	-34.9 ± 1.2	11.9 ± 0.8
Phase II (day 150-240)	R4.35	no	555 ± 62.3	306 ± 36.7	55.0 ± 1.7	44.7 ± 1.7	7.41 ± 0.13	2.14 ± 0.07	83.66 ± 38.44	56.03 ± 27.80	-35.6 ± 2.4	13.3 ± 0.7
	R4.36	γ-HCH (50 µM)	536 ± 66.1	287 ± 36.5	55.5 ± 1.4	44.2 ± 1.4	7.42 ± 0.10	2.02 ± 0.17	155.72 ± 78.27	89.70 ± 37.71	-34.9 ± 1.5	11.9 ± 0.9
Phase III (day 240-330)	R4.35	no	557 ± 73.9	311 ± 43.2	55.7 ± 1.8	43.9 ± 1.9	7.50 ± 0.07	2.22 ± 0.05	55.21 ± 23.32	37.47 ± 13.48	-33.2 ± 2.5	12.6 ± 1.4
	R4.36	α -HCH (50 µM)	568 ± 77.0	308 ± 44.2	55.8 ± 1.6	43.8 ± 1.7	7.49 ± 0.07	2.15 ± 0.10	183.64 ± 91.82	98.48 ± 36.41	-34.2 ± 2.9	12.3 ± 1.5
Phase IV (day 330-380)	R4.35	no	507 ± 67.6	266 ± 31.8	54.9 ± 2.2	44.5 ± 2.6	7.52 ± 0.14	2.22 ± 0.03	216.92 ± 35.82	117.40 ± 8.54	-36.9 ± 2.9	13.3 ± 1.6
	R4.36	β-HCH (50 µM)	545 ± 87.4	283 ± 39.4	55.4 ± 2.0	44.0 ± 2.4	7.56 ± 0.11	2.20 ± 0.04	151.60 ± 128.19	79.98 ± 61.47	-34.5 ± 6.5	13.7 ± 1.2

Table 1 Operating conditions and parameters of CSTRs

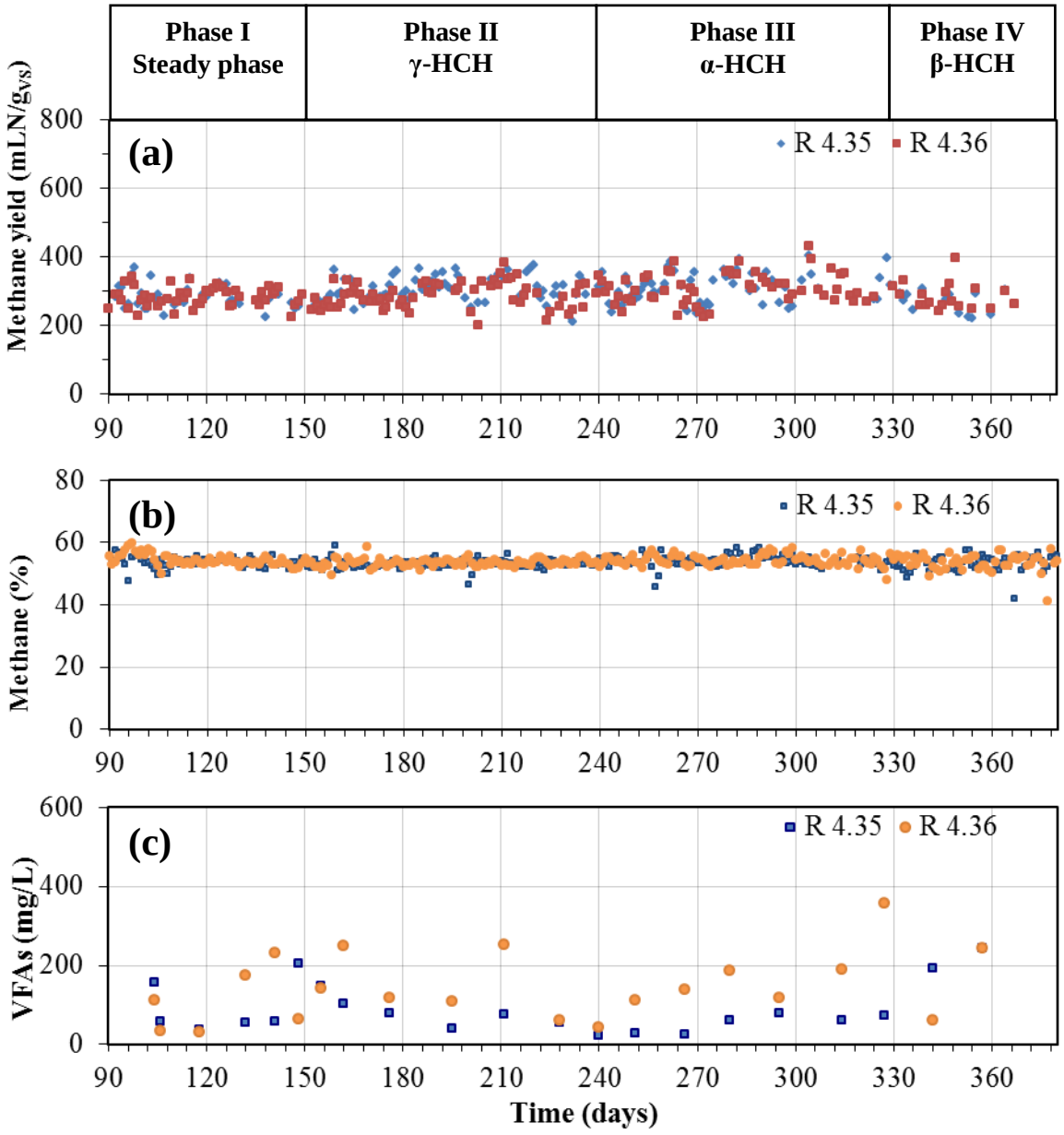

677

678 **Fig. 1** Methane yield (a), methane content (b) and total VFAs (c) in CSTRs over phases I to IV.

679 Data were corrected to pressure (101.325 kPa) and standard temperature (273.15 k), thus are

680 reported as normalized milliliters (mL_N) per gram of volatile solid (VS).

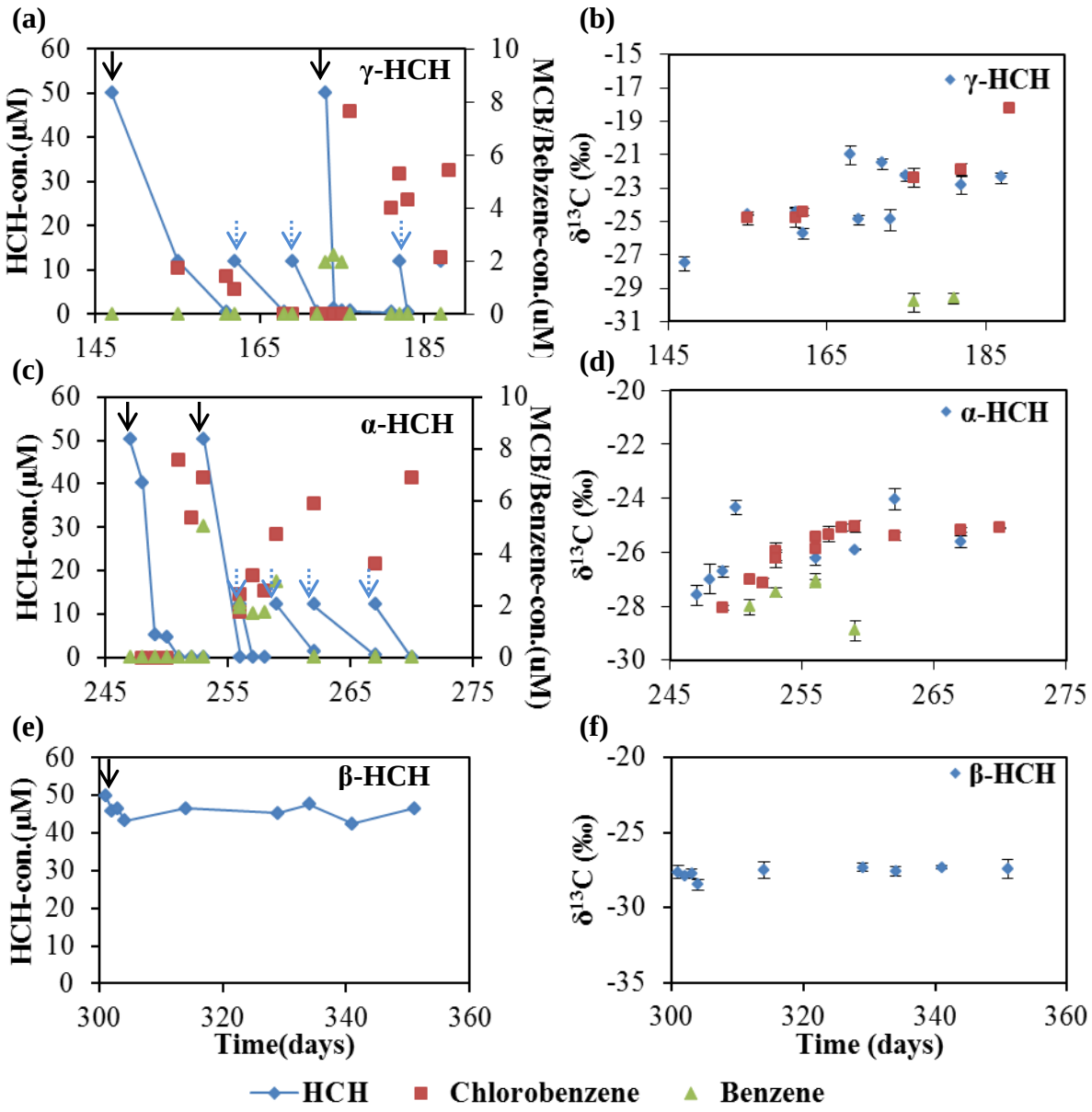

681 **Fig. 2** Concentrations and carbon isotope compositions of γ-HCH (a&b), α-HCH (c&d), β-HCH
682 (e&f) and metabolites (chlorobenzene and benzene). Values of 0 indicate that they were below
683 the detection limit. Black arrows mean adjustment of the concentration to 50 μM and blue
684 arrows represent the addition of HCH to 12 μM. Values of $\delta^{13}C$ are associated with
685 concentration and the data below the confidential interval of detection via GC-IRMS are not
686 shown here.

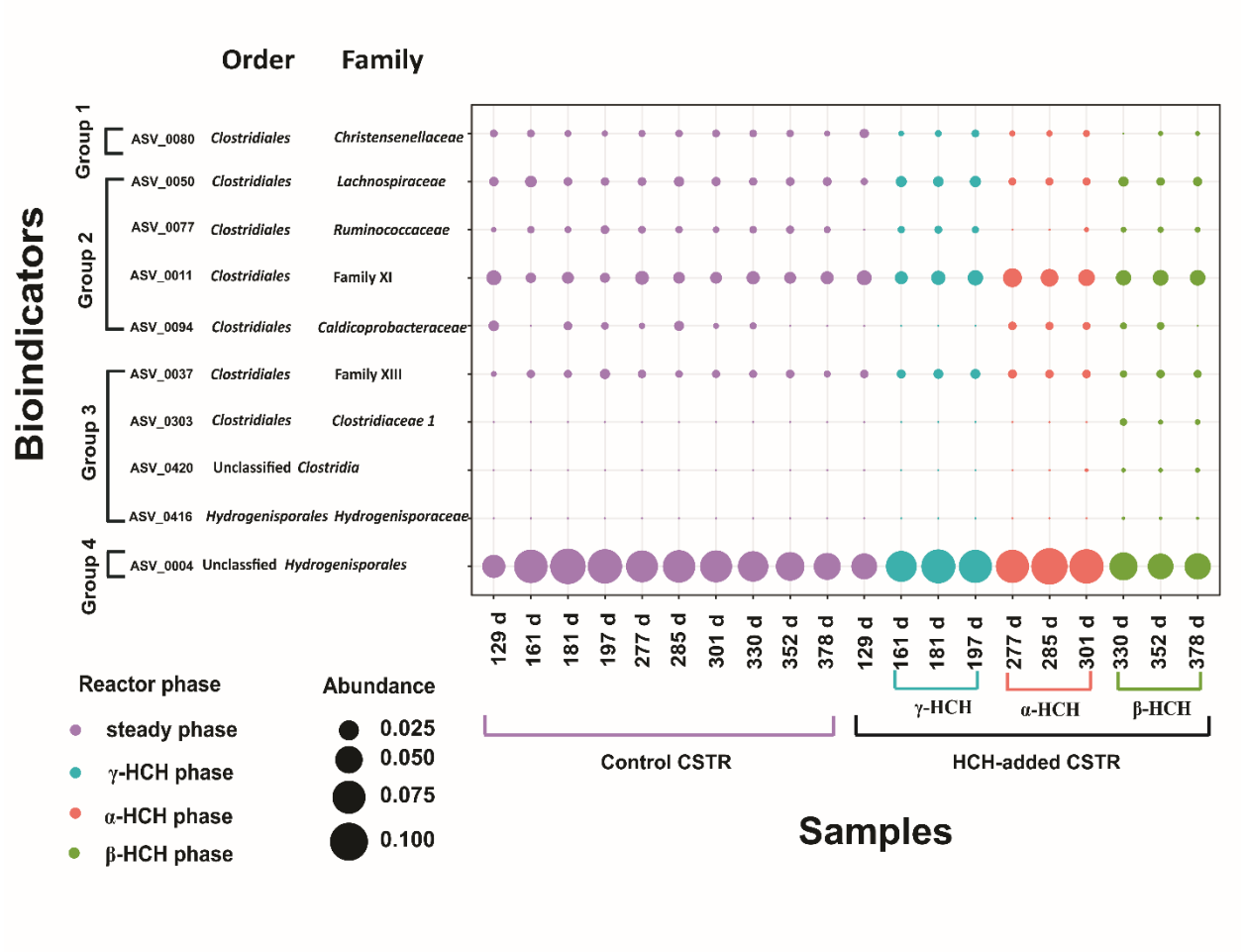

687

688 **Fig. 3** Relative abundance distribution of ASVs used as bioindicators in the control CSTR and

689 HCH-added CSTR.

690 ASVs separated in 4 different groups depending on statistic differences ($P < 0.05$) of abundance

691 using the LSMEANS test with FDR multiple correction, based on the interaction of pairwise

692 reactor phases: steady phase vs. β-HCH phase (Group1); γ-HCH phase vs. α-HCH phase

693 (Group2); γ-HCH phase vs. β-HCH phase (Group3); α-HCH phase vs. β-HCH phase (Group4).

694

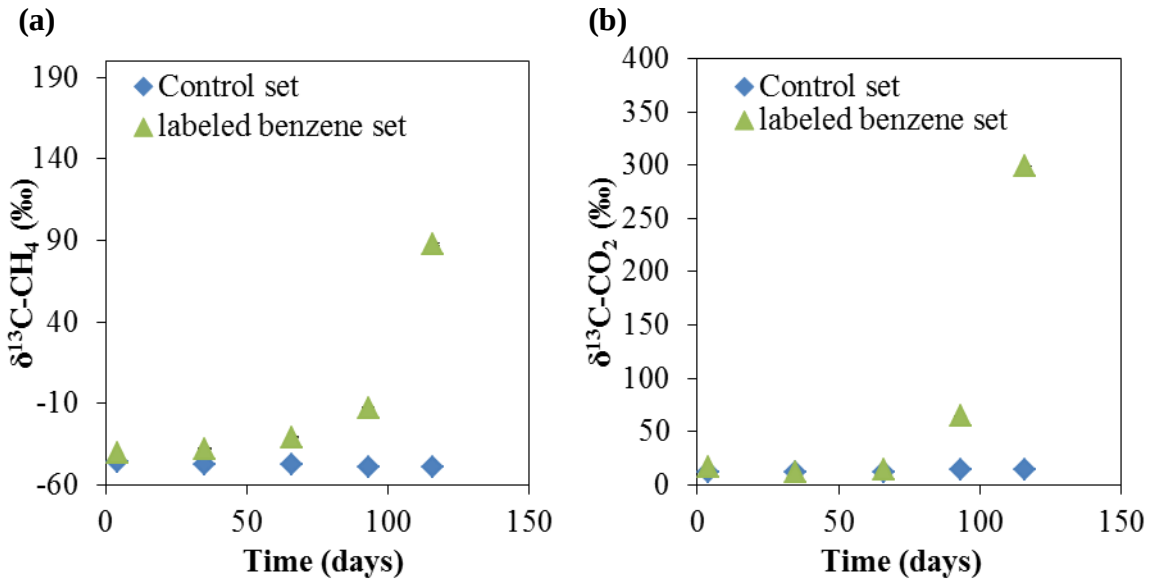

695

696 **Fig. 4** Carbon isotope signatures of methane (a) and CO_2 (b) in batch experiment with addition

697 of benzene-$^{13}C_6$.

698

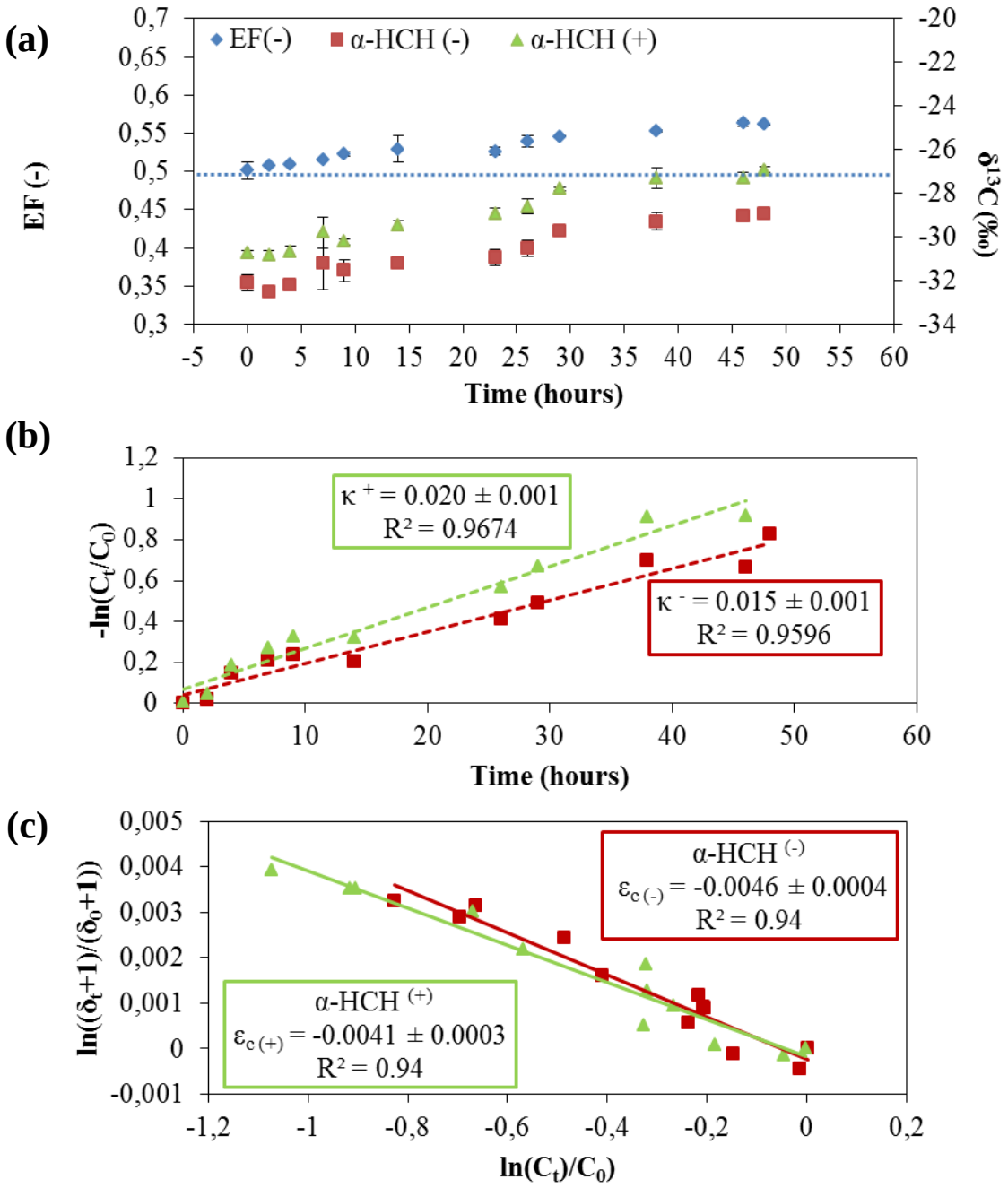

699 **Fig. 5** Enantiomer fractionation (EF) of (-) α-HCH and carbon isotope compositions of (-) / (+)

700 α-HCH in biogas slurry (batch experiment) (a)**;** the degradation kinetics of (-) α-HCH (◆) and

701 (+) α-HCH (■) in biogas slurry (b); carbon stable isotope enrichment factors of (-) / (+) α-HCH

702 (c).

703 **Scheme 1** Proposed interaction between anaerobic digestion and HCH dehalogenation with

704 subsequent mineralization

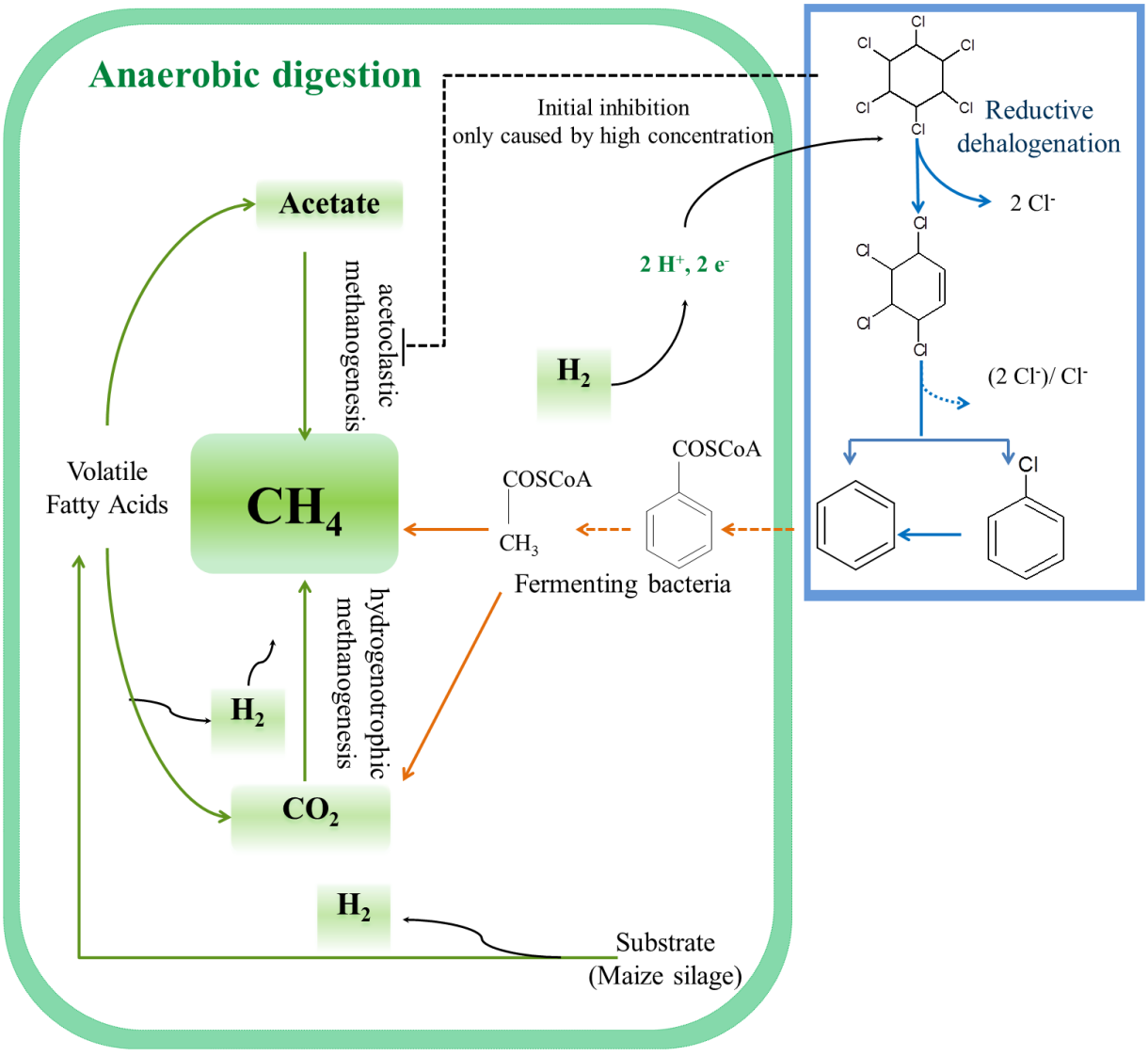

705

***Novelty Statement (maximum limit:100 words)**

We provide a concept for characterization of the transformation of hexachlorocyclohexanes (HCH)-contaminated biomass with anaerobic digestion (AD) to produce biogas in a 15 L continuous flow reactor. The parameters are needed for upscaling. The transformation during the AD process was analyzed by isotope fractionation analysis of HCH isomers (γ, α and β) and the enantiomeric fractionation of α-HCH. The response of the microbial community to HCH addition was analyzed by molecular microbiology and isotope composition of the CH_4 and CO_2. The reactor showed a robust conversion to biogas when loaded with HCH in concentration typical for contaminated biomass.

.

Referees:

Prof. Dr. Ralf Conrad (Director)
Max-Planck-Institut für terrestrische Mikrobiologie
Karl-von-Frisch-Straße 10, D-35043 Marburg, Germany
Phone: +49 6421 178 801. Fax: +49 642 178 999
E-mail: conrad@mpi-marburg.mpg.de
(Top expert on isotope fractionation and methanogenesis, methanogenic pathways)

Prof. Dr. Frank Keppler
Institut für Geowissenschaften
Im Neuenheimer Feld 236, Raum 202
D-69120 Heidelberg
Phone: +49 (0) 6221 546009
E-Mail: frank.keppler@geow.uni-heidelberg.de
(Geochemist and expert in isotope fingerprinting of methanogenesis, isotope fractionation to characterize the methane cycle)

Prof. Elizabeth A. Edwards
Dept. of Chemical Engineering and Applied Chemistry
University of Toronto
200 College Street, Toronto, ON, M5S 3E5, Canada
Phone: 416 946 3506, Fax: 416 978 8605
Email: elizabeth.edwards@utoronto.ca
(Microbiologist: Expert in microbiology, degradation of contaminants)

Prof. Théodore Bouchez
Microbial Biotechnologies
National Research Institute of Science and Technology for Environment and Agricultural, France
1 rue Pierre-Gilles de Gennes, CS 10030, F-92761 Antony Cedex, France
Phone: (+33) 140966040; Fax: (+33) 140966072.
E-mail theodore.bouchez@cemagref.fr
(Expert on anaerobic digestion)

Prof. Gumersindo Feijoo
Department of Chemical Engineering, School of Engineering
Rúa Lope Gómez de Marzoa s/n University of Santiago de Compostela
E-15782 Santiago de Compostela, Spain
Phone: +34 881816776/Fax: +34 881816702
E-mail: Gumersindo.feijoo@usc.es
(Expert on bioremediation and biodegradation of pesticides in bioreactors)

Prof. Irini Angelidaki

Department of Environmental Engineering, Technical University of Denmark
DK-2800, Kgs Lyngby, Denmark
Phone: +45 45 25 14 29, Mobile: +45 30 61 38 89, Fax: +45 45 93 28 50
E-mail: iria@env.dtu.dk
(Expert on anaerobic digestion)

Highlight

1. A pollution clean-up strategy combines phytoremediation and anaerobic digestion.
2. Hexachlorocyclohexane (HCH) contaminated plant was used as substrate for biogas reactor.
3. No negative influence on biogas yield was caused by HCHs.
4. Microbial community structure was influenced by HCH addition.
5. HCHs can be transformed to benzene and chlorobenzene and further mineralized.

Supplementary Material A

Click here to download Supplementary Material: Appendix_A_Supplementary material-final-19-09-2019.docx

Appendix B

Click here to download Supplementary Material: Appendix_B_SupplementaryTableA-4-28-6-19.xlsx

Appendix C

Click here to download Supplementary Material: Appendix_C_SupplementaryTableA-5_28-06-19.xlsx

Appendix D

Click here to download Supplementary Material: Appendix_D_SupplementaryTableA.6_ASV -10.09.2019-final.xlsx

Appendix E

Click here to download Supplementary Material: Appendix_E_SupplementaryTableA.7_Taxonomy_ASVs-10.09.2019-final.xlsx

Supplementary Material G

Click here to download Supplementary Material: Appendix G.pdf

Supplementary Material F

Click here to download Supplementary Material: Apendix F.pdf

Biotransformation of hexachlorocyclohexanes contaminated biomass for energetic utilization demonstrated in continuous anaerobic digestion system

Shujuan Lian[a], Marcell Nikolausz*[b], Ivonne Nijenhuis[a], Ulisses Nunes da Rocha[b], Bin Liu[b], Felipe Borim Corrêa[b], João Pedro Leonor Fernandes Saraiva[b] and Hans Hermann Richnow*[a]

[a] Department of Isotope Biogeochemistry, Helmholtz Centre for Environmental Research - UFZ, Permoserstraße 15, 04318 Leipzig, Germany

(E-mail: shujuan.lian@ufz.de, ivonne.nijenhuis@ufz.de, hans.richnow@ufz.de)

[b] Department of Environmental Microbiology, Helmholtz Centre for Environmental Research - UFZ, Permoserstraße 15, 04318 Leipzig, Germany

(E-mail: marcell.nikolausz@ufz.de, ulisses.rocha@ufz.de, bin.liu@ufz.de, felipe.correa@ufz.de, joao.saraiva@ufz.de)

*Corresponding authors:

Hans Hermann Richnow, Tel.: +49 341 2351 212; E-mail: hans.richnow@ufz.de

Marcell Nikolausz, Tel.: +49 341 243 4566; E-mail: marcell.nikolausz@ufz.de

Abstract

Lindane, the γ-hexachlorocyclohexane (HCH) isomer, was among the most used pesticides worldwide. Although it was banned in 2009, residues of Lindane and other HCH-isomers are still found with high concentrations in contaminated fields. For clean-up, phytoremediation combined with anaerobic digestion (AD) of contaminated biomass to produce biogas and fertilizer could be a promising strategy and was tested in two 15 L laboratory-scale continuous-stirred-tank-reactors. During operation over one year by adding HCH isomers (γ, α and β) consecutively, no negative influence on conventional reactor parameters was observed. The γ- and α-HCH isomers were transformed to chlorobenzene and benzene, and transformation became faster along with time, while β-HCH was not removed. Genus *Methanosaeta* and order *Clostridiales*, showing significant enhancement on abundance with HCH addition, may be used as bioindicators for HCH dehalogenation in AD process. The potential for HCH degradation in AD system was restricted to axial Cl atoms of HCH and it showed slight enantioselective preference towards transformation of (+) α-HCH. Moreover, metabolite benzene was mineralized to CO_2 and methane, deducing from tracer experiments with benzene-$^{13}C_6$. Overall, AD appears to be a feasible option for treatment of γ and α-HCHs contaminated biomass.

Key words: Hexachlorocyclohexane; anaerobic digestion; stable isotope; reductive dehalogenation; cleanup strategy

1. Introduction

Contamination by Persistent Organic Pollutants (POPs) prevents further utilization of arable lands for food and feed production. However, such lands may still be utilized for growth of energy crops with degradation properties such as wheat or other plants [1,2]. Potentially the contaminated biomass can be used as feedstock for anaerobic digestion (AD) to produce biogas as energy carrier and for use of the digestate as fertilizer. Thus, we propose a strategy combing phytoremediation with AD of hexachlorocyclohexane (HCH) contaminated biomass to produce biogas and still retain soil fertility, which might be a model for other halogenated POPs.

Huge amounts of Lindane, γ-HCH, have been used as pesticide worldwide until banned in the Stockholm convention 2009, due to the toxic and carcinogenic effects on human health and adverse environmental issues [3]. However HCHs are still found at high concentrations worldwide in areas of former pesticide production, since other HCH-isomers as by-products of Lindane production were dumped at production sites [4]. Plants and crops grown on contaminated land can accumulate HCH [5], which is a potential entry of HCH to food webs. Concentration between 1 and 10 µg g^{-1} dry weight plant biomass has been found in the vicinity contaminated site [2] which is far above the acceptable levels and raises concerns when used as a food stock. However, contaminated biomass after phytoremediation [6,7] might be used for biogas production and opens an option for using polluted land [8]. Therefore, for clean-up, phytoremediation can be used in the contaminated field and the HCH-contaminated biomass can be used as substrate of AD for biogas production.

An understanding on the fate of HCHs in AD is required for the full-scale application. Anaerobic degradation processes metabolize pollutants through reductive pathways with mineralization or

reduction of highly electrophilic halo- and nitro-groups, to less toxic compounds by transferring electrons to the contaminant [9–11]. Particularly reductive dehalogenation is favored under anoxic conditions. Thus, HCH as persistent halogenated organic contaminants can be transformed through reductive dehalogenation under anaerobic condition [12–16] and also in biogas system as it was demonstrated in our recent study [8].

The transformation of HCHs during wastewater treatment in up-flow anaerobic sludge blanket reactor (UASB) had been also reported [17,18]. However, the fate of HCH during continuous large-scale AD with plant biomass feedstock and its effect on reactor performance during biogas production was not yet investigated. According to our previous study with batch reactors [8], HCH addition up to 150 mg/L has no negative influence on final methane yield from main substrate and the transformation rates of γ- and α-HCH were high, which demonstrated that AD appears to be a bioremediation option for HCH contaminated biomass.

For this work, we scaled up the AD process to bio-transform HCH in continuous mode, for characterization of the transformation processes as required before utilizing contaminated biomass in large-scale for biogas production. Therefore, a continuous stirred tank reactor (CSTR) was established to investigate the interaction of HCHs and microbiota in larger scale in semi-continuous feeding mode.

The transformation pathway of HCHs can be identified employing metabolite formation and compound-specific stable isotope analysis (CSIA) [19–22]. Fractionation factors of HCH can then be used for comparison with culture studies for characterisation of the transformation pathway in AD process [23–26]. Moreover, assessment of the main methanogenic pathways in biogas reactors [27–30] can be deduced from isotope composition of the produced methane [31–

36]. In addition, batch experiment with ^{13}C-labelled benzene was conducted for investigation of the complete mineralisation of HCHs to CH_4 and CO_2.

Overall, we evaluated the potential application of AD system for treatment of HCH-contaminated biomass in a technical laboratory-scale CSTR. The specific objectives of this study were to: (i) monitor the convential operation of CSTR with addition of HCH isomers (γ, α and β); (ii) prove the potential application of AD for treatment of HCH-contaminated biomass in continuous reactor mode; (iii) characterize the biotransformation pathways of HCHs and the effect of various isomers on microbiota in AD; (iv) show the potential conversion of HCHs to methane and CO_2 in AD system.

2. Materials and Methods

2.1. Substrate and Inoculum

Maize silage (Total solids (TS) = 25.47%, VS (volatile solids) = 96.51% of TS) was used as substrate. The inoculum (TS = 3.41%, VS = 72.20% TS) was sieved biogas slurry taken from the main reactor of a pilot-scale biogas plant which used maize silage and cattle manure as substrate with an organic loading rate (OLR) of 3.5 $g_{vs}L^{-1}day^{-1}$ and hydraulic retention time (HRT) of 47 days. HCH isomers (γ-, α- and β-HCH, separately, analytical purity of 99%) and hexachlorobenzene (HCB) (Lot 60119, analytical purity of 99%), were obtained from Sigma-Aldrich (Munich, Germany). Final concentration of HCH (each isomer) in the reactors was set as 50 μM based on the literature value [37] and our previous inhibition experiment [8] to reflect some potential real case scenarios.

2.2. Setup of CSTRs

Two laboratory-scale CSTRs were operated over more than one year under mesophilic condition (38-40℃) with maize silage as exclusive substrate. One reactor (reactor R4.36) with HCH addition was set up to investigate the interaction of HCH with microbiota; another reactor (reactor R4.35) was operated as the control experiment without addition of HCH. The total reactor volume was 15 L with 10 L working volume. The whole running period was divided into 4 stages for R4.36 after the start-up: the steady phase for establishing the biogas process (phase I), the addition of γ-HCH (phase II), the addition of α-HCH (phase III) and the addition of β-HCH (phase IV) (details of reactor setup see **section A.1.1., Appendix A**).

2.3. Sampling procedure and operating parameters analysis of CSTR

The biogas was collected in a gas bag which was connected to a gas meter TG 05 (Ritter, Germany), then transferred to an AwiFlex gas analyzer (Awite Bioenergie GmbH, Germany) for gas composition measurement [38]. Biogas samples for isotope analysis were taken from the headspace of CSTRs weekly before daily addition of maize silage. They were collected in triplicates using 10-ml gas-tight vacuumed vials for carbon isotope composition [33].

Effluent liquid was periodically collected from both reactors at the same time: (i) 50 mL liquid were stored in 120 mL serum bottle at -20 ℃ for extraction of HCH and its metabolites, to measure the concentration and carbon isotope composition. The detailed protocol was described in our previous publication [8]. (ii) Another 50 mL were taken weekly and centrifuged at 10,000 × g, 10 ℃ for 10 min and filtered with a mesh sieve of 1 mm. The filtrate was used for analysis of volatile fatty acid (VFA) and total ammonia nitrogen (TAN) (details of analysis on parameters see **section A.1.2., Appendix A**).

2.4. Microbial community structure analysis

Triplicate 0.5 mL samples were taken from both CSTRs periodically and stored at -20 ℃ for molecular biological analysis. Three samplings for each phase with single HCH isomer were conducted (day 129 for steady phase; days 161, 181 and 197 for γ-HCH phase; days 277 and 301 for α-HCH phase; days 330, 352 and 378 for β-HCH phase). The total genomic DNA was extracted with 'NucleoSpin Soil' kit (Macherey-Nagel GmbH & Co. KG, Düren, Germany) according to the manufacturer's protocol using buffer SL2 with enhancer SX.

The 16S rRNA genes were further amplified and sequenced via Illumina$^{@}$ MiSeq. Shannon index and amplicon sequence variant (ASV) counts (α-diversity) were determined using the R package phyloseq [39]. Differences in bacterial community composition (β-diversity) were calculated using Bray–Curtis dissimilarity index based on rarefied (15063 ASV counts per sample) and square-root-transformed ASV abundances, which are demonstrated via nonmetric multi-dimensional scaling (NMDS) plot. Permutational multivariate analysis of variance (PERMANOVA) [40] were calculated by "adonis2" function in "vegan" R package using 10^6 permutations to determine if different environmental variables (i.e., time, HCH addition and reactor phases) were important factors correlated with shifts in ASV abundance. Further, ASVs which could be used to classify the difference of HCH-added and non-added reactors between reactor phases were identified (hereafter, bioindicators). In order to determine bioindicators, the analyzes were conducted with three steps [41]. First, machine learning derived from Random Forest [42] to calculate variable important ASVs via Mean Decrease Gini for reactor phase and other important factors from the NMDS analysis. Second, the potential bioindicators were those ASVs that only present on machine learning of reactor phase deducting the ASVs that both relevant for reactor phase and other important factors. Third, bioindicators were identified from

147 the above selected ASVs removing those were not statistically significant via the LSMEANS test
148 with pair-wise methods adjusted by false discovery rate (FDR) correction [43,44].

149 The diversity of microbial communities from both reactors was also investigated by terminal
150 restriction fragment length polymorphism (T-RFLP) analysis of methyl-coenzyme M reductase
151 alpha-subunit (*mcrA*) genes for archaea and the variable regions V1–V3 of bacterial 16S rRNA
152 gene fragments for bacteria [45–48].

153 **2.5. Batch experiments with labelled benzene-$^{13}C_6$ in AD**

154 For evaluating further degradation of the HCH metabolite benzene, labelled compound (benzene-
155 $^{13}C_6$) with final concentration of 100 µM was spiked with a glass syringe as pure compound into
156 serum bottles filled with 50 ml slurry taken from the benzene-added set of automatic methane
157 potential test system (AMPTS, Bioprocess Control Sweden AB, Sweden) described in our
158 previous study [8]. The preparation was done in an anaerobic glove box (gas atmosphere—N_2:H_2
159 (95:5); Coy Laboratory Products Inc., USA). Control set was prepared simultaneously in
160 triplicate only with slurry from benzene-added set.

161 **2.6. Enantioselectivity and Enantiomer-specific stable isotope fractionation of α-HCH**

162 In order to derive enantioselectivity (ES), 21.8 mg/L (75 µmol/L) of α-HCH were added
163 respectively into 120 mL bottles with 50 mL biogas digestate from CSTR effluent. The
164 headspace was flushed with nitrogen for 5 min before the bottles were closed with Teflon™-
165 coated butyl rubber septa and crimped. Fifteen parallel bottles for each isomer were prepared for
166 sampling at different time points. (details on calculation of ES see **section A.1.5., Appendix A**).
167 In addition, triplicate negative controls with sterilized digestate and α-HCH were conducted. In

the sterilized control concentration remain stable and no metabolites were detected, showing that biotransformation only occurred in active biogas digestate (data not shown).

3. Results

3.1. Performance of CSTRs

3.1.1. Methane production, total ammonium nitrogen and volatile fatty acids for characterization of AD processes

In phase I (steady phase), the average specific methane production (SMP) was 286 ± 32.1 and 283 ± 27.7 mL_N/g VS in the control reactor and the reactor later used for HCH supplementation, respectively, and were statistically identical. After addition of γ-HCH in phase II, SMPs were 287 ± 36.5 and 306 ± 36.7 mL_N/g VS in the control and HCH-added reactor, respectively; in phase III, the SMPs were 311 ± 43.2 and 308 ± 44.2 mL_N/g VS in control and α-HCH reactors, respectively; in phase IV, SMPs of 266 ± 31.8 and 283 ± 39.4 mL_N/g VS were observed in control and β-HCH reactors, respectively (**Fig. 1a and Table 1**). The SMPs were statistically identical in both reactors during phase I to IV, indicating addition of HCHs did not affect the SMP. Methane and CO_2 contents were 54~56% and 43~45%, respectively, during the whole running period (**Fig. 1b**).

In start-up phase, concentrations of VFAs and acetate were 95.1 ± 68.5 and 66.4 ± 45.1 mg/L for control reactor, respectively (108.4 ± 81.2 and 64.8 ± 42.4 mg/L for HCH-added reactor). In phase II and III (γ-HCH and α-HCH phase), the concentrations of VFAs and acetate were generally slightly higher in HCH-added reactor compared to the control reactor (**Fig. 1c** and **Fig. A.2**). In general, there was a significant difference between concentrations of VFAs in these two

reactors (p-value= 0.02187, $p < 0.05$; one way ANOVA analysis), nevertheless all these values were still within conventional ranges of stable operation.

3.1.2. Concentration and stable isotope analysis for biotransformation of HCHs

Concentrations and stable isotope compositions of HCHs and the metabolites are shown in **Fig. 2**. In phase II (day 147-187), the addition of HCH was about 50 µM for the whole reactor. Both γ- and α-HCH were nearly completely removed within 14 days and 7 days, respectively. The γ-HCH degraded faster after day 173 with a removal below the limit of detection within 3 days. Similarly, in phase III (day 245-275), α-HCH transformed faster at day 253 compared to addition at day 245. In phase II and III, benzene and MCB were detected as metabolites. No transformation of β-HCH was detected in phase IV of our system from day 330 to day 360, which was deduced from the constant concentration and lack of metabolites.

Carbon isotope enrichment of γ-HCH and α-HCH was observed from -27.5 to -21.0‰ and from -27.5 to -24.0‰, respectively (**Fig. 2**). The variations were in a similar order with respect to the isotope enrichment of $\delta^{13}C$ observed in our previous study from-27.5 to -17.0‰ for γ-HCH and from -27.5 to -23.0‰ for α-HCH [8], however the number of data do not allow quantifying the isotope fractionation using the Rayleigh approach in the continuous flow reactor. The $\delta^{13}C$ values of β-HCH were stable at ca. -27.5‰ in phase IV. The $\delta^{13}C$ values of chlorobenzene ranged from -24.8 to -18.2‰ in γ-HCH phase and from -28.1 to -25.1‰ in α-HCH phase, showing same increasing tendency as HCH isomers. Whereas $\delta^{13}C$ values of benzene was ranging from -29.8 to -27.2‰ but the isotope measurement of this metabolite was only possible in few samples, due to the low concentrations (**Fig. 2**).

3.1.3. Microbial community structure

NMDS plots for bacterial microbial community structures of all selected samples in both reactors are shown in **Fig. A.5**. In the PERMANOVA main test (**Table A.2**), significant difference (Pseudo-F = 2.25788, P = 0.004693, **Fig. A.5b**) was observed between the two reactors taken the reactor phase as a factor. Although, no significant difference was shown between both reactors taking HCH addition as a factor (Pseudo-F = 1.64138, P = 0.095825, **Fig. A.5b**) we observed statistically significant differences when comparing the different reactor phases to the control samples collected in the same dates (**Fig. A.5.c-e**). In addition, time was also found as important factor between early and late phases with the significant difference (Pseudo-F = 9.07219 and P = 0.000012) (**Fig. A.5a**). For identification of the bioindicators which could differentiate HCH-added reactor and control reactor responding to reactor phase, three steps were conducted. First, as reactor phase and time both were important factors, 35 variable important ASVs were selected for each of them based on random forest analysis (**Fig. A.6** & **A.7**). Moreover, confusion matrices were generated for classification of the samples using the rarefied ASV relative abundances as numeric values with time, HCH-addition and HCH phase as factors (**Table A.1**). Second, 28 ASVs were obtained as potential bioindicators relevant to reactor phase rather than time after machine learning (**Table A.3**). Third, 10 ASVs significantly different ($P < 0.05$) to reactor phase via the LSMEANS test by FDR multiple correction (**Appendix B** & **C**) selected from last two steps, were identified as bioindicators. Boxplots were used for every chosen bioindicator to depict statistically different ($P < 0.05$) contribution of ASVs caused by addition of different HCH isomer in HCH-added reactor and control reactor (**Fig. A.8**). To demonstrate ASVs which were significantly associated with the pairwise reactor phases ($P < 0.05$) (**Fig. 3**), these ASVs were separated into four groups: steady phase vs. β-HCH phase (Group1); γ-HCH

phase vs. α-HCH phase (Group2); γ-HCH phase vs. β-HCH phase (Group3); α-HCH phase vs. β-HCH phase (Group4). Among the 10 ASVs identified as bioindicators, 8 ASVs are classified to order *Clostridiales*, which provide the relations of HCH addition with the abundance of *Clostridiales*. The other 2 ASVs are assigned to order *Hydrogenisporales*.

The variation of methanogens in control reactor and HCH-added reactor at different phases was demonstrated via T-RFLP (**Fig. A.9**). The bacterial and archaeal community compositions in both reactors converged toward different direction in intra-sample variability NMDS plots (**Fig. A.10**). Significant difference was observed in archaea between the control reactor and HCH-added reactor (PERMANOVA main test; pseudo-F = 2.986, P = 0.015, see also **Fig. A.10a**). However, no significant difference was observed in bacteria from the NMDS plots (PERMANOVA main test; pseudo-F = 2.205, P >0.05, see also **Fig. A.10b**). The correlation between the communities and reactor parameters is depicted as arrows in the NMDS plots. The direction and length of arrow which represents the abundance of genus *Methanosaeta* showed strong correlation with HCH addition. Furthermore, concentration of acetate was also correlated with addition of HCH solution (**Fig. A.2a**).

Taking both results from MiSeq and T-RFLP into consideration, HCH-added reactor had a higher abundance of *Methanosaeta* and *Clostridiales* compared to the control reactor. The isotope signature of methane indicates an increase in acetoclastic methanogens, correlating with the increased *Methanosaeta*.

3.2. Labelled benzene-$^{13}C_6$ degradation in AD system

The further degradation and mineralization of benzene was observed in the microcosms prepared with slurry from a benzene supplemented batch system of our previous study and amended with

255 $^{13}C_6$-labelled benzene. Significant amounts of ^{13}C labelled CO_2 ($\delta^{13}C$ = +299.0 ± 0.2‰) and

256 methane ($\delta^{13}C$ = 87.3 ± 0.4‰) were detected after 116 days (**Fig. 4**), which is a direct evidence

257 for the conversion of labelled benzene $^{13}C_6$ to CO_2 and methane. Meanwhile, in control set the

258 carbon stable isotope composition of methane and CO_2 remained stable at -48.8 ± 1.3 ‰ and

259 14.4 ± 0.3 ‰, respectively.

260 The slurry from benzene-added set of AMPTS was also sequenced via Illumina@ MiSeq.

261 Microbes, such as class *Spirochaetes*, class *Epsilonproteobacteria*, order *Thermotogales*, family

262 *Peptococcaceae*, genera *Pelotomaculum* and *Desulfosporosinus*, potentially associated with

263 benzene degradation [49–53] were found in benzene amended slurry from our system (see

264 **Appendix D** & **E**).

265 **3.3.Enantiomer fractionation (EF) and enantiomer-specific isotope fractionation of α-HCH**

266 **in batch experiment**

267 In the sterilized control experiment, $\delta^{13}C$ values of (-) and (+) α-HCH were stable at -31.9 ± 0.5

268 and -30.7 ± 0.2‰, respectively; the concentration remained constant at ca. 75 µmol/L, showing

269 that no abiotic transformation took place. In active biogas slurry, $\delta^{13}C$ values of (-) and (+) α-

270 HCH were both enriched, ranging from -32.1 ± 0.4 to -29.3 ± 0.4‰ and from -30.7 ± 0.1 to -26.9

271 ± 0.1‰, respectively **(Fig. 5a**). According to Rayleigh equation, carbon isotope fractionation

272 factors (ε_c) of (+) and (-) *α*-HCH are -4.1 ± 0.3‰ and -4.6 ± 0.4‰, respectively (**Fig. 5c**).

273 Simultaneously, EF of (-) α-HCH increased from 0.50 to 0.56. The degradation kinetics of (-) α-

274 HCH and (+) α-HCH in biogas slurry with values of 0.015 ± 0.001 and 0.020 ± 0.001are shown

275 in **Fig. 5b**, suggesting preferential transformation of (+) α-HCH in AD system. Similar trend was

276 also observed in CSTR and the EF of (-) α-HCH was shifted to 0.57 (**Fig. A.11**). The

277 enantiomeric fractionation was consistent with the enantioselectivity observed in the batch
278 experiment. Thus, (+) α-HCH was preferentially transformed in AD system and can be used as
279 an indicator for biodegradation.

280 **4. Discussion**

281 **4.1. Effect of HCHs on the performance of CSTR**

282 The typical concentration of HCH in plants near the HCH dumpsite was found up to 29 $\mu g \cdot g^{-1}$[2].
283 Concentrations amended in CSTR (50 μM, equal to 243 $\mu g \cdot g^{-1}$) was higher; however, no
284 significant differences in both SBP and SMP were observed between two reactors in all phases
285 with $P > 0.05$. Control and HCH-added reactor had similar pH, TAN concentrations, as well as
286 the content of methane and CO_2; however, relatively higher concentrations of VFAs were
287 detected in the HCH-added reactor, which might be attributed to the addition of HCH. Overall,
288 the conventional parameters in CSTRs had no significant fluctuation caused by HCH-addition at
289 concentration of 50 μM, indicating the potential for treatment of HCH contaminated biomass in
290 AD system under continuous mode. The quality of the maize silage used as the main substrate
291 for feeding was not constant; therefore, it had also influence on the gas production values, but it
292 affected both reactors in a similar way.

293 **4.2. Bioindicators responding to HCH addition in the microbial communities of CSTR**

294 **4.2.1. Dynamics of the bacterial community**

295 Reductive dehalogenation has been proven as main pathway of HCHs transformation in AD
296 system [8], suggesting HCHs as electron acceptors can be co-metabolized by microorganisms.
297 Despite the similar process parameters in the experimental and control reactors, addition of
298 respective HCH isomers in different reactor phases had a significant effect on the microbial

community structures. The communities were classified with confidence up to Genus level due to the size of the amplicon in this study; however, groups belonging to the same taxonomic/phylogenetic group have similar functions. ASVs belonging to order *Clostridiales* were identified as bioindicator responding to HCH-addition, due to the significant variation on abundance. Moreover, ASVs belonging to the class *Dehalococcoidia*, a taxon containing organohalide respiring bacteria [9,54,55], were also found in our system already in the initial phase (see **Appendix D** & **E**). This highlights the intrinsic potential of the AD microbiota to deal with halogenated compounds. Acetogenic bacteria and *Clostridium* sp. were found to be linked to reductive dehalogenation of HCHs in other studies [56,57]. Reductive dechlorination of Lindane was also detected from cell-free extracts *of Clostridium rectum* [58] and *Clostridium sphenoides* [59].

4.2.2. Dynamics of the methanogenic community

The dominant methanogens were affiliated to genus *Methanoculleus* in both reactors (**Fig. A.9**). Species affiliated to *Methanoculleus* were dominant methanogens in many biogas-producing reactor systems fed with maize silage and manure [60]. Although this hydrogenotrophic methanogen was predominant in both reactors, the abundance in HCH-added reactor was lower than in control reactor. These small coccoid methanogens are sensitive to detergents, physical and osmotic stresses [61], which might explain the reduced relative abundance of *Methanoculleus* in the experimental reactor after HCHs solution was added.

A significant increase of the abundance of genus *Methanosaeta* in the HCH-added reactor was detected, and it is consistent with the bioindicators derived from Miseq analysis and NMDS plots. The enriched $\delta^{13}C\text{-}CH_4$ caused by β-HCH addition also confirmed the increased abundance of putative acetotrophic methanogens (**Fig. A.9**). It was reported that *Methanosaeta* spp.

outcompeted *Methanosarcina* spp.as acetotrophic methanogens when acetate concentrations were lower than 200 mg L^{-1} [62], similar to observations in this study. *Methanosaeta* and *Methanosarcina* spp. were dominant methanogens in anaerobic reactors treating wastewater with other halogenated compounds such as tetrachloroethylene and 2-chlorophenol [63,64]. Genus *Methanosaeta* comprises anaerobic, nonmotile, non-sporeforming rods with flat ends in morphology and it can form flexible filaments in a continuous, tubular, proteinaceous sheath for resisting harmful chemical agents [65]. Thus, it was assumed that its cell envelope structure was conducive to resist the toxicity of HCHs, which resulted in increased predominance of *Methanosaeta* in HCH-added reactor.

4.3. Biodegradation of HCH to biogas

4.3.1. Biotransformation of HCH to benzene and chlorobenzene in AD

In this study, we proved the biotransformation of HCH not only from the decrease in concentration and the detection of metabolites, but also from the stable isotope compositions of HCH and metabolites, which provides a new unambiguous analysis method for biotransformation of chemicals in AD system. In conventional studies, the indication on biodegradation of chemicals was deduced from the reduced concentration during the reaction period, which is a controversial issue since absorption and volatilization of chemicals in AD slurry can also lead to the decrease of concentration. Biotransformation of HCH can be confirmed from the reduced concentration and enriched carbon isotope composition of HCH during γ and α-HCH reactor phase, as well as from detection of metabolites and the enrichment of carbon isotope composition of chlorobenzene.

4.3.2. Mineralization of labelled benzene-$^{13}C_6$ to biogas

The formation of labelled methane and CO_2 from benzene proved that the detected HCH metabolites benzene can be further degraded. The benzene mineralization to CO_2 and methane under methanogenic conditions was reported [51,66–68], however were not detected in AD systems before. The putative pathway of benzene is proposed starting with the conversion of benzene to phenol by hydroxylation or to toluene by methylation [69] and subsequent transformation to benzoate [70]. Further degradation can be achieved via benzoyl-CoA pathway [71].

The conversion of total amount of benzene to CH_4 was estimated, to evaluate the contribution of benzene degradation to enhancement on methane yield. If there is 100% conversion of 100 µmol benzene, ca. 9.2 mL methane will be produced. The calculation was based on the equation below [72], which is calculated with CO_2 as electron acceptor under methanogenic conditions:

$$4C_6H_6 + 27H_2O \rightarrow 15CH_4 + 9HCO_3^- + 9H^+ \ldots\ldots \quad \textbf{(Eq. 2)}$$

In case of current biomass conversion AD systems, a long storage of digestate is required by the authorities to avoid the residual methane production and its negative climate effect. The retention time in such digestate storage facilities usually exceed 100 days, which would provide the time needed to completely degrade the remaining metabolites benzene to biogas.

To evaluate the interaction of AD and HCHs, the proposed linked pathways during full degradation of α and γ HCH in biogas-producing system is summarized in **Scheme 1**. AD provided the reductive condition for dehalogenation of HCH with H_2 or acetate, produced during fermentation, as electronic donor. Furthermore, the metabolite benzene was mineralized to biogas in AD. HCH with concentration higher than 150 mg/L can cause temporary inhibition on

acetoclastic methanogenesis [8]. In CSTR setup, HCH contaminated plants showed no negative influence on methane production. In general, α and γ HCH can be degraded to methane and CO_2 in AD systems, indicating the positive potential of HCH-contaminated biomass for biogas production not only from plant substrate but also from the contaminant HCH.

4.4.Structure selectivity of HCHs in anaerobic digestion

4.4.1. Diastereoselectivity of HCHs

The isomers of HCHs denoted by Greek letters (α, β, γ, δ, ε, η, and θ, see **section A.1**, **Appendix A**) differ in their axial- equatorial substitution pattern around the ring [73]. In our previous study, it was assumed that transformation mechanism of HCHs in AD system was reductive dehalogenation [8]. In this study, α, β and γ isomers were tested in CSTR system, among which, γ isomer possessing three axial Cl atoms transformed faster than the α isomer with two axial Cl atoms. Subsequently, no transformation of β isomer without axial Cl atom was observed in AD system. Thus, it was assumed that dihaloelimination or anti-periplanar dehydrochlorination occurs to eliminate sequentially chlorine resulting in the final metabolites as chlorobenzene and benzene [8,15,74]. The transformed order of HCH isomers in our study is consistent with the report of Buser *et al* [74]. The results suggest that the transformation rate of HCH in AD system was associated with the number of axial Cl, since axial atoms are easier to be cleaved from the parent compound than equatorial Cl atoms.

4.4.2. Enantioselectivity of α-HCH

Enantioselectivity for α-HCH in biogas reactor is significantly different from the aerobic degradation in research by Bashir *et al* [25]. Variation of (EF) (−), from 0.45 to 0.14 in *Sphingobium indicum* strain B90A and 0.50 to 0.24 for *Sphingobium indicum* strain UT26, was

discovered, indicating that (-) α-HCH was preferentially degraded in oxic condition [25]. Contrarily, EF (-) changed from 0.50 to 0.56, which was associated with slight preference towards the transformation of (+) α-HCH in our AD system. The ES values of 0.14 is different from the aerobic transformation by *Sphingobium indicum* strain B90A with ES of -0.45 [21]. However, no enantioselectivity of α-HCH during the reductive dehalogenation by the *Dehalococcoides mccartyi* strains in anoxic condition was observed [22]. In contrast, the enantio-selectivity in this study is consistent as reported by Buser and Müller with the faster degradation of (+) α-HCH compared to (-)α-HCH in sewage sludge [74].

5. Conclusion and outlook

The addition of HCHs in CSTR showed no negative influence on conventional reactor parameters and methanogenesis at the concentration range found in biomass grown on contaminated areas. The robust microbiota of AD process can adapt to the toxic HCH isomers and even successful biodegrade γ and α isomers. In addition, benzene can be degraded to methane and CO_2, deduced from the isotope labelling test, indicating the potential full conversion of HCHs to biogas with long retention time of post digestion. The isotope and enantiomer fractionation can be used to characterize the transformation in AD systems. The isotope fractionation pattern of HCH might be used to evaluate the process and the isotope fractionation pattern of CH_4 and CO_2 to monitor the status of the AD reactor. In summary, phytoremediation coupled to AD and subsequent fertilization using digestate is a promising strategy for economic use and simultaneous remediation of POPs contaminated lands.

Conflicts of interest

There are no conflicts to declare.

Acknowledgements

Shujuan Lian was funded by the China Scholarship Council [File No. 201404910520] and supported by the Helmholtz Interdisciplinary Graduate School for Environmental Research. The experimental setup of AMPTS and CSTR was supported by DBFZ (German Biomass Research Centre). We acknowledge the financial support from the German-Israeli Foundation for Research and Development (GIF) Grant no. I-1368-307.8/2016 ("Prediction of chiral and isotope enrichment during the transformations of halo-organic pollutants: Mechanistic and QSAR approaches"). Thanks to Ute Lohse for supplying help with microbial analysis. Thanks to Steffen Kümmel for helping with isotope measurements and to Monika Möder for freeze-drying samples. And thanks to Rodolfo Brizola Toscan for helping with data process of MiSeq. Dr. Ulisses Nunes da Rocha and Dr. Joao Pedro Saraiva are financed by the Helmholtz Association VH-NG-1248 Micro 'Big Data'. The study was supported by the Initiative and Networking Fund of the Helmholtz Association.

Appendix A. Supplementary material

Supplementary material associated with this article can be found, in the online version.

Appendix B. Supplementary Table A.4

Supplementary Table A.4 associated with this article can be found, in the online version.

Appendix C. Supplementary Table A.5

Supplementary Table A.5 associated with this article can be found, in the online version.

Appendix D. Supplementary Table A.6

Supplementary Table A.6 associated with this article can be found, in the online version.

Appendix E. Supplementary Table A.7

Supplementary Table A.7 associated with this article can be found, in the online version.

Appendix F. Xiao Liu et al., 2019; manuscript in review, for review only

Appendix G. Yaqing Liu et al., 2019; manuscript in review, for review only

Figure captions

Fig. 1 Methane yield (a), methane content (b) and total VFAs (c) in CSTRs over phases I to IV. Data were corrected to pressure (101.325 kPa) and standard temperature (273.15 k), thus are reported as normalized milliliters (mLN) per gram of volatile solid (VS).

Fig. 2 Concentrations and carbon isotope compositions of γ-HCH (a&b), α-HCH (c&d), β-HCH (e&f) and metabolites (chlorobenzene and benzene). Values of 0 indicate that they were below the detection limit. Black arrows mean adjustment of the concentration to 50 μM and blue arrows represent the addition of HCH to 12 μM. Values of $\delta^{13}C$ are associated with concentration and the data below the confidential interval of detection via GC-IRMS are not shown here.

Fig. 3 Relative abundance distribution of ASVs used as bioindicators in the control CSTR and HCH-added CSTR per sample.

ASVs separated in 4 different groups depending on statistic differences ($P < 0.05$) of abundance using the LSMEANS test with FDR multiple correction, based on the interaction of pairwise reactor phases: steady phase vs. β-HCH phase (Group1); γ-HCH phase vs. α-HCH phase (Group2); γ-HCH phase vs. β-HCH phase (Group3); α-HCH phase vs. β-HCH phase (Group4).

Fig. 4 Carbon isotope signatures of methane (a) and CO_2 (b) in batch experiment with addition of benzene-$^{13}C_6$.

Fig. 5 Enantiomer fractionation (EF) of (-) α-HCH and carbon isotope compositions of (-) / (+) α-HCH in biogas slurry (batch experiment) (a); the degradation kinetics of (-) α-HCH (◆) and (+) α-HCH (■) in biogas slurry (b); carbon stable isotope enrichment factors of (-) / (+) α-HCH (c).

References

[1] X. Liu, L. Wu, S. Kümmel, H. Richnow, Characterizing the biotransformation of hexachlorocyclohexane in wheat using compound-specific stable isotope analysis and enantiomer fraction analysis, (2019) submitted, see Appendix F, manuscript in review.

[2] L. Wu, Y. Liu, X. Liu, A. Bajaj, M. Sharma, R. Lal, H. Richnow, Isotope fractionation approach to characterize the reactive transport processes governing the fate of hexachlorocyclohexanes at a contaminated site in India, Environ. Int. 132 (2019) 105036.

[3] J. Vijgen, P.C. Abhilash, Y.F. Li, R. Lal, M. Forter, J. Torres, N. Singh, M. Yunus, C. Tian, A. Schäffer, R. Weber, Hexachlorocyclohexane (HCH) as new Stockholm Convention POPs-a global perspective on the management of Lindane and its waste isomers, Environ. Sci. Pollut. Res. 18 (2011) 152–162.

[4] W. Slooff, A. Matthijsen, J. Canton, H. Eerens, C. van Gestel, E. Heijna-Merkus, P. Greve, P. Janssen, J. van Koten-Vermeulen, J. Knoop, Integrated criteria document hexachlorocyclohexanes, 1988.

[5] L. Wu, S. Moses, Y. Liu, J. Renpenning, H.H. Richnow, A concept for studying the transformation reaction of hexachlorocyclohexanes in food webs using multi-element compound-specific isotope analysis, Anal. Chim. Acta. 1064 (2019) 56–64.

[6] S. Hussain, T. Siddique, M. Arshad, M. Saleem, Bioremediation and phytoremediation of pesticides: recent advances, Crit. Rev. Environ. Sci. Technol. 39 (2009) 843–907.

[7] N. Agrawal, S.K. Shahi, An environmental cleanup strategy - microbial transformation of xenobiotic compounds, Int. J. Curr. Microbiol. Appl. Sci. 4 (2015) 429–461.

[8] S. Lian, M. Nikolausz, I. Nijenhuis, A.F. Leite, H.H. Richnow, Biotransformation and inhibition effects of hexachlorocyclohexanes during biogas production from contaminated biomass characterized by isotope fractionation concepts, Bioresour. Technol. 250 (2018) 683–690.

[9] T. Kaufhold, M. Schmidt, D. Cichocka, M. Nikolausz, I. Nijenhuis, Dehalogenation of diverse halogenated substrates by a highly enriched *Dehalococcoides*-containing culture derived from the contaminated mega-site in Bitterfeld, FEMS Microbiol. Ecol. 83 (2013) 176–188.

[10] J. Ye, A. Singh, O.P. Ward, Biodegradation of nitroaromatics and other nitrogen-containing xenobiotics, World J. Microbiol. Biotechnol. 20 (2004) 117–135.

[11] K.J. Rockne, K.R. Reddy, W.T. Street, Bioremediation of contaminated sites, in: Int. e-Conference Mod. Trends Found. Eng. Geotech. Challenges Solut., 2003: pp. 1–22.

[12] I. V. Robles-González, E. Ríos-Leal, I. Sastre-Conde, F. Fava, N. Rinderknecht-Seijas, H.M. Poggi-Varaldo, Slurry bioreactors with simultaneous electron acceptors for bioremediation of an agricultural soil polluted with Lindane, Process Biochem. 47 (2012) 1640–1648.

[13] S. Bashir, K.L. Hitzfeld, M. Gehre, H.H. Richnow, A. Fischer, Evaluating degradation of hexachlorcyclohexane (HCH) isomers within a contaminated aquifer using compound-specific stable carbon isotope analysis (CSIA), Water Res. 71 (2015) 187–196.

[14] P.J.M. Middeldorp, M. Jaspers, A.J.B. Zehnder, G. Schraa, Biotransformation of α-, β-, γ-, and δ -hexachlorocyclohexane under methanogenic conditions, Environ. Sci. Technol. 30

(1996) 2345–2349.

[15] R. Lal, G. Pandey, P. Sharma, K. Kumari, S. Malhotra, R. Pandey, V. Raina, H.E. Kohler, C. Holliger, C. Jackson, J.G. Oakeshott, Biochemistry of microbial degradation of hexachlorocyclohexane and prospects for bioremediation, Microbiol. Mol. Biol. Rev. 74 (2010) 58–80.

[16] P.J.M. Middeldorp, W. Van Doesburg, G. Schraa, A.J.M. Stams, Reductive dechlorination of hexachlorocyclohexane (HCH) isomers in soil under anaerobic conditions, Biodegradation. 16 (2005) 283–290.

[17] T.P. Baczynski, J. Kurbiel, Identification of operational parameters critical for removal of selected chlorinated pesticides in UASB reactor, Proc. 9th World Congr. Anaerob. Dig. Anaerob. Convers. Sustain. 1 (2001).

[18] P. Bhatt, M.S. Kumar, S.N. Mudliar, T. Chakrabarti, Biodegradation of tech-hexachlorocyclohexane in a upflow anaerobic sludge blanket (UASB) reactor, Bioresour. Technol. 97 (2006) 824–830.

[19] C. Wiegert, Application of two dimensional compound specific carbon-chlorine isotope analyses for degradation monitoring and assessment of organic pollutants in contaminated soil and groundwater, Dr. Thesis, Stock. Univ. (2013).

[20] S.A. Law, T.F. Bidleman, M.J. Martin, Evidence of enantioselective degradation of α-hexachlorocyclohexane in groundwater, Env. Sci Technol. 38 (2004) 1633–1638.

[21] Y. Liu, L. Wu, P. Kohli, R. Kumar, H. Stryhanyuk, I. Nijenhuis, R. Lal, H.-H. Richnow, Enantiomer and carbon isotope fractionation of α-hexachlorocyclohexane by *Sphingobium*

indicum strain B90A and the corresponding enzymes, Environ. Sci. Technol. 53 (2019) 8715-8724.

[22] Y. Liu, J. Liu, J. Renpenning, I. Nijenhuis, H.-H. Richnow, Dual C-Cl isotope analysis for characterizing the reductive dechlorination of α- and γ-hexachlorocyclohexane by two *Dehalococcoides mccartyi* strains and an Enrichment culture, (2019) submitted, see Appendix G, manuscript in review.

[23] S.L. Badea, C. Vogt, S. Weber, A.F. Danet, H.H. Richnow, Stable isotope fractionation of γ-hexachlorocyclohexane (Lindane) during reductive dechlorination by two strains of sulfate-reducing bacteria, Environ. Sci. Technol. 43 (2009) 3155–3161.

[24] S.L. Badea, C. Vogt, M. Gehre, A. Fischer, A.F. Danet, H.H. Richnow, Development of an enantiomer-specific stable carbon isotope analysis (ESIA) method for assessing the fate of α-hexachlorocyclohexane in the environment, Rapid Commun. Mass Spectrom. 25 (2011) 1363–1372.

[25] S. Bashir, A. Fischer, I. Nijenhuis, H.H. Richnow, Enantioselective carbon stable isotope fractionation of hexachlorocyclohexane during aerobic biodegradation by *Sphingobium* spp., Environ. Sci. Technol. 47 (2013) 11432–11439.

[26] S. Bashir, Assessment of in situ transformation of Hexachlorocyclohexane using carbon stable isotope analysis (CSIA) (Doctoral dissertation), Eberhard Karls Universität Tübingen, 2014.

[27] D. Polag, L.C. Krapf, H. Heuwinkel, S. Laukenmann, J. Lelieveld, F. Keppler, Stable carbon isotopes of methane for real-time process monitoring in anaerobic digesters, Eng.

Life Sci. 14 (2014) 153–160.

[28] D. Polag, T. May, L. Müller, H. König, F. Jacobi, S. Laukenmann, F. Keppler, Online monitoring of stable carbon isotopes of methane in anaerobic digestion as a new tool for early warning of process instability, Bioresour. Technol. 197 (2015) 161–170.

[29] Z. Lv, M. Hu, H. Harms, H.H. Richnow, J. Liebetrau, M. Nikolausz, H. Hermann, J. Liebetrau, M. Nikolausz, Stable isotope composition of biogas allows early warning of complete process failure as a result of ammonia inhibition in anaerobic digesters, Bioresour. Technol. 167 (2014) 251–259.

[30] J. De Vrieze, M. De Waele, P. Boeckx, N. Boon, Isotope fractionation in biogas allows direct microbial community stability monitoring in anaerobic digestion, Environ. Sci. Technol. 52 (2018) 6704–6713.

[31] J.A. Krzycki, W.R. Kenealy, M.J. Deniro, J.G. Zeikusl, Stable carbon isotope fractionation by *Methanosarcina barkeri* during methanogenesis from acetate, methanol, or carbon dioxide-hydrogen, Appl. Environ. Microbiol. 53 (1987) 2597–2599.

[32] R. Conrad, Quantification of methanogenic pathways using stable carbon isotopic signatures: A review and a proposal, Org. Geochem. 36 (2005) 739–752.

[33] S. Laukenmann, D. Polag, M. Greule, A. Gronauer, Identification of methanogenic pathways in anaerobic digesters using stable carbon isotopes, Eng. Life Sci. 10 (2010) 509–514.

[34] P.E. Galand, K. Yrjälä, R. Conrad, Stable carbon isotope fractionation during methanogenesis in three boreal peatland ecosystems, Biogeosciences. 7 (2010) 3893–3900.

[35] H. Penning, P. Claus, P. Casper, R. Conrad, Carbon isotope fractionation during acetoclastic methanogenesis by *Methanosaeta concilii* in culture and a lake sediment, Appl. Environ. Microbiol. 72 (2006) 5648–5652.

[36] E.R.C. Hornibrook, F.J. Longstaffe, W.S. Fyfe, Evolution of stable carbon isotope compositions for methane and carbon dioxide in freshwater wetlands and other anaerobic environments, Geochim. Cosmochim. Acta. 64 (2000) 1013–1027.

[37] J.C. Quintero, M.T. Moreira, J.M. Lema, G. Feijoo, An anaerobic bioreactor allows the efficient degradation of HCH isomers in soil slurry, Chemosphere. 63 (2006) 1005–1013.

[38] D.G. Mulat, H.F. Jacobi, A. Feilberg, A.P.S. Adamsen, H.-H. Richnow, M. Nikolausz, Changing feeding regimes to demonstrate flexible biogas production: effects on process performance, microbial community structure, and methanogenesis pathways, Appl. Environ. Microbiol. 82 (2016) 438–449.

[39] P.J. McMurdie, S. Holmes, phyloseq: an R package for reproducible interactive analysis and graphics of microbiome census data, PLoS One. 8 (2013) 1–11.

[40] M.J. Anderson, Permutational multivariate analysis of variance (PERMANOVA), Wiley StatsRef Stat. Ref. Online. (2017) 1–15.

[41] P.M. Rosado, D.C.A. Leite, G.A.S. Duarte, R.M. Chaloub, G. Jospin, U. Nunes da Rocha, J. P. Saraiva, F. Dini-Andreote, J.A. Eisen, D.G. Bourne, R.S. Peixoto, Marine probiotics: increasing coral resistance to bleaching through microbiome manipulation, ISME J. (2018) Published: 05 December 2018.

[42] A. Liaw, M. Wiener, Classification and regression by randomForest, R News. 2/3 (2002)

18–22.

[43] A. V. Longo, K.R. Zamudio, Environmental fluctuations and host skin bacteria shift survival advantage between frogs and their fungal pathogen, ISME J. 11 (2017) 349–361.

[44] R. V. Lenth, Least-squares means: the R package lsmeans, J. Stat. Softw. 69 (2016) 1–33.

[45] T. Lueders, K.J. Chin, R. Conrad, M. Friedrich, Molecular analyses of methyl-coenzyme M reductase α-subunit (*mcrA*) genes in rice field soil and enrichment cultures reveal the methanogenic phenotype of a novel archaeal lineage, Environ. Microbiol. 3 (2001) 194–204.

[46] J.D. Neufeld, W.W. Mohn, V. De Lorenzo, Composition of microbial communities in hexachlorocyclohexane (HCH) contaminated soils from Spain revealed with a habitat-specific microarray, Environ. Microbiol. 8 (2006) 126–140.

[47] N. Sangwan, P. Lata, V. Dwivedi, A. Singh, N. Niharika, J. Kaur, S. Anand, J. Malhotra, S. Jindal, A. Nigam, D. Lal, A. Dua, A. Saxena, N. Garg, M. Verma, J. Kaur, U. Mukherjee, J.A. Gilbert, S.E. Dowd, R. Raman, P. Khurana, J.P. Khurana, R. Lal, Comparative metagenomic analysis of soil microbial communities across three hexachlorocyclohexane contamination levels, PLoS One. 7 (2012) 1–12.

[48] M.J. Whiticar, E. Faber, M. Schoell, Biogenic methane formation in marine and freshwater environments: CO_2 reduction vs acetate fermentation - isotope evidence, Geochim. Cosmochim. Acta. 50 (1986) 693–709.

[49] M. Nales, B.J. Butler, E.A. Edwards, Anaerobic benzene biodegradation: a microcosm survey, Bioremediat. J. 2 (1998) 125–144.

[50] J.N. Rooney-varga, R.T. Anderson, J.L. Fraga, D.R. Lovley, Microbial communities associated with anaerobic benzene degradation in a petroleum-contaminated aquifer, Appl. Environ. Microbiol. 65 (1999) 3056–3063.

[51] C. Vogt, S. Kleinsteuber, H.H. Richnow, Anaerobic benzene degradation by bacteria, Microb. Biotechnol. 4 (2011) 710–724.

[52] S. Atashgahi, B. Hornung, M.J. van der Waals, U. Nunes da Rocha, F. Hugenholtz, B. Nijsse, D. Molenaar, R. van Spanning, A.J.M. Stams, J. Gerritse, H. Smidt, A benzene-degrading nitrate-reducing microbial consortium displays aerobic and anaerobic benzene degradation pathways, Sci. Rep. (2018) 1–12.

[53] M.J. van der Waals, C. Pijls, A.J.C. Sinke, A.A.M. Langenhoff, H. Smidt, J. Gerritse, Anaerobic degradation of a mixture of MtBE, EtBE, TBA, and benzene under different redox conditions, Appl. Microbiol. Biotechnol. 102 (2018) 3387–3397.

[54] B. Matturro, C. Ubaldi, S. Rossetti, Microbiome dynamics of a polychlorobiphenyl (PCB) historically contaminated marine sediment under conditions promoting reductive dechlorination, Front. Microbiol. 7 (2016) 1–14.

[55] S. Bashir, K. Kuntze, C. Vogt, I. Nijenhuis, Anaerobic biotransformation of hexachlorocyclohexane isomers by *Dehalococcoides* species and an enrichment culture, Biodegradation. 29 (2018) 409–418.

[56] B. Camacho-Pérez, E. Ríos-Leal, N. Rinderknecht-Seijas, H.M. Poggi-Varaldo, Enzymes involved in the biodegradation of hexachlorocyclohexane: a mini review, J. Environ. Manage. 95 (2012) S306–S318.

[57] C. Holliger, G. Schraa, Physiological meaning and potential for application of reductive dechlorination by anaerobic bacteria, FEMS Microbiol. Rev. 15 (1994) 297–305.

[58] N. Ohisa, M. Yamaguchil, N. Kurihara, Lindane degradation by cell-free extracts of Clostridium rectum, Arch. Microbiol. 225 (1980) 221–225.

[59] A.D. Heritage, I.C. Macrae, Degradation of Lindane by cell-free preparations of *Clostridium sphenoides*, Appl. Environ. Microbiol. 34 (1977) 222–224.

[60] I. Maus, D. Wibberg, R. Stantscheff, F.G. Eikmeyer, A. Seffner, J. Boelter, R. Szczepanowski, J. Blom, S. Jaenicke, H. König, A. Pühler, A. Schlüter, Complete genome sequence of the hydrogenotrophic, methanogenic archaeon *Methanoculleus bourgensis* strain MS2T, isolated from a sewage sludge digester, J. Bacteriol. 194 (2012) 5487–5488.

[61] G.M. Maestrojuán, D.R. Boone, L. Xun, R.A. Mah, L. Zhang, Transfer of *Methanogenium bourgens*e, *Methanogenium marisnigri*, *Methanogenium olentangyi*, and *Methanogenium thermophilicum* to the genus *Methanoculleus* gen. nov., emendation of *Methanoculleus marisnigri* and *Methanogenium*, and description of new strains of *Methanoculleus bourgense* and *Methanoculleus marisnigri*., Int. J. Syst. Bacteriol. 40 (2009) 117–122.

[62] D. Zheng, L. Raskin, Quantification of *Methanosaeta* species in anaerobic bioreactors using genus- and species-specific hybridization probes, Microb. Ecol. 39 (2000) 246–262.

[63] S.M. Prakash, S.K. Gupta, Biodegradation of tetrachloroethylene in upflow anaerobic sludge blanket reactor, Bioresour. Technol. 72 (2000) 47–54.

[64] L. Beristain-Montiel, S. Martínez-Hernández, F. de M. Cuervo-López, F. Ramírez-Vives, Dynamics of a microbial community exposed to several concentrations of 2-chlorophenol

in an anaerobic sequencing batch reactor, Environ. Technol. 36 (2015) 1776–1784.

[65] Girishchandra B. Patel, G.D. Sprott, *Methanosaeta concilii* gen. nov., sp. nov. ("*Methanothrix concilii*") and *Methanosaeta thermoacetophila* nom, rev., comb. nov., Int. J. Syst. Bacteriol. 40 (1990) 79–82.

[66] J. Kazumi, M.E. Caldwell, J.M. Suflita, D.R. Lovley, L.Y. Young, Anaerobic degradation of benzene in diverse anoxic environments, Environ. Sci. Technol. 31 (1997) 813–818.

[67] X. Liang, C.E. Devine, J. Nelson, B. Sherwood Lollar, S. Zinder, E.A. Edwards, Anaerobic conversion of chlorobenzene and benzene to CH_4 and CO_2 in bioaugmented microcosms, Environ. Sci. Technol. 47 (2013) 2378–2385.

[68] M. Schmidt, D. Wolfram, J. Birkigt, J. Ahlheim, H. Paschke, H.H. Richnow, I. Nijenhuis, Iron oxides stimulate microbial monochlorobenzene in situ transformation in constructed wetlands and laboratory systems, Sci. Total Environ. 472 (2014) 185–193.

[69] S.A. Mancini, C.E. Devine, M. Elsner, M.E. Nandi, A.C. Ulrich, E.A. Edwards, B.S. Lollar, Isotopic evidence suggests different initial reaction mechanisms for anaerobic benzene biodegradation, Environ. Sci. Technol. 42 (2008) 8290–8296.

[70] M.E. Caldwell, J.M. Suflita, Detection of phenol and benzoate as intermediates of anaerobic benzene biodegradation under different terminal electron-accepting conditions, Environ. Sci. Technol. 34 (2000) 1216–1220.

[71] C.S. Harwood, G. Burchhardt, H. Herrmann, G. Fuchs, Anaerobic metabolism of aromatic compounds via the benzoyl-CoA pathway, FEMS Microbiol. Rev. 22 (1998) 439–458.

[72] J.M. Weiner, D.R. Lovley, Rapid benzene degradation in methanogenic sediments from a

667 petroleum-contaminated aquifer, Appl. Environ. Microbiol. 64 (1998) 1937–1939.

668 [73] K.L. Willett, E.M. Ulrich, R.A. Hites, Differential toxicity and environmental fates of
669 hexachlorocyclohexane isomers, Environ. Sci. Technol. 32 (1998) 2197–2207.

670 [74] H.R. Buser, M.D. Müller, Isomer and enantioselective degradation of
671 hexachlorocyclohexane isomers in sewage sludge under anaerobic conditions, Environ.
672 Sci. Technol. 29 (1995) 664–672.

673

Phase	Reactor	HCH addition	SBP (mL_N/g VS)	SMP (mL_N/g VS)	Methane (%)	CO_2 (%)	pH	TAN (NH^{4+}-N/L)	VFAs (mg/L)	Acetate (mg/L)	$\delta^{13}C$-CH_4 (‰)	$\delta^{13}C$-CO_2 (‰)
Phase I (day 90-150)	R4.35	no	511 ± 57.7	286 ± 32.1	55.9 ± 2.1	43.7 ± 2.2	7.41 ± 0.09	1.90 ± 0.17	95.14 ± 68.54	66.38 ± 45.07	-35.7 ± 1.2	11.7 ± 0.5
	R4.36	no	505 ± 51.2	283 ± 27.7	55.9 ± 1.9	43.8 ± 2.0	7.41 ± 0.08	1.90 ± 0.17	108.37 ± 81.21	64.84 ± 42.42	-34.9 ± 1.2	11.9 ± 0.8
Phase II (day 150-240)	R4.35	no	555 ± 62.3	306 ± 36.7	55.0 ± 1.7	44.7 ± 1.7	7.41 ± 0.13	2.14 ± 0.07	83.66 ± 38.44	56.03 ± 27.80	-35.6 ± 2.4	13.3 ± 0.7
	R4.36	γ-HCH (50 µM)	536 ± 66.1	287 ± 36.5	55.5 ± 1.4	44.2 ± 1.4	7.42 ± 0.10	2.02 ± 0.17	155.72 ± 78.27	89.70 ± 37.71	-34.9 ± 1.5	11.9 ± 0.9
Phase III (day 240-330)	R4.35	no	557 ± 73.9	311 ± 43.2	55.7 ± 1.8	43.9 ± 1.9	7.50 ± 0.07	2.22 ± 0.05	55.21 ± 23.32	37.47 ± 13.48	-33.2 ± 2.5	12.6 ± 1.4
	R4.36	α -HCH (50 µM)	568 ± 77.0	308 ± 44.2	55.8 ± 1.6	43.8 ± 1.7	7.49 ± 0.07	2.15 ± 0.10	183.64 ± 91.82	98.48 ± 36.41	-34.2 ± 2.9	12.3 ± 1.5
Phase IV (day 330-380)	R4.35	no	507 ± 67.6	266 ± 31.8	54.9 ± 2.2	44.5 ± 2.6	7.52 ± 0.14	2.22 ± 0.03	216.92 ± 35.82	117.40 ± 8.54	-36.9 ± 2.9	13.3 ± 1.6
	R4.36	β-HCH (50 µM)	545 ± 87.4	283 ± 39.4	55.4 ± 2.0	44.0 ± 2.4	7.56 ± 0.11	2.20 ± 0.04	151.60 ± 128.19	79.98 ± 61.47	-34.5 ± 6.5	13.7 ± 1.2

Table 1 Operating conditions and parameters of CSTRs

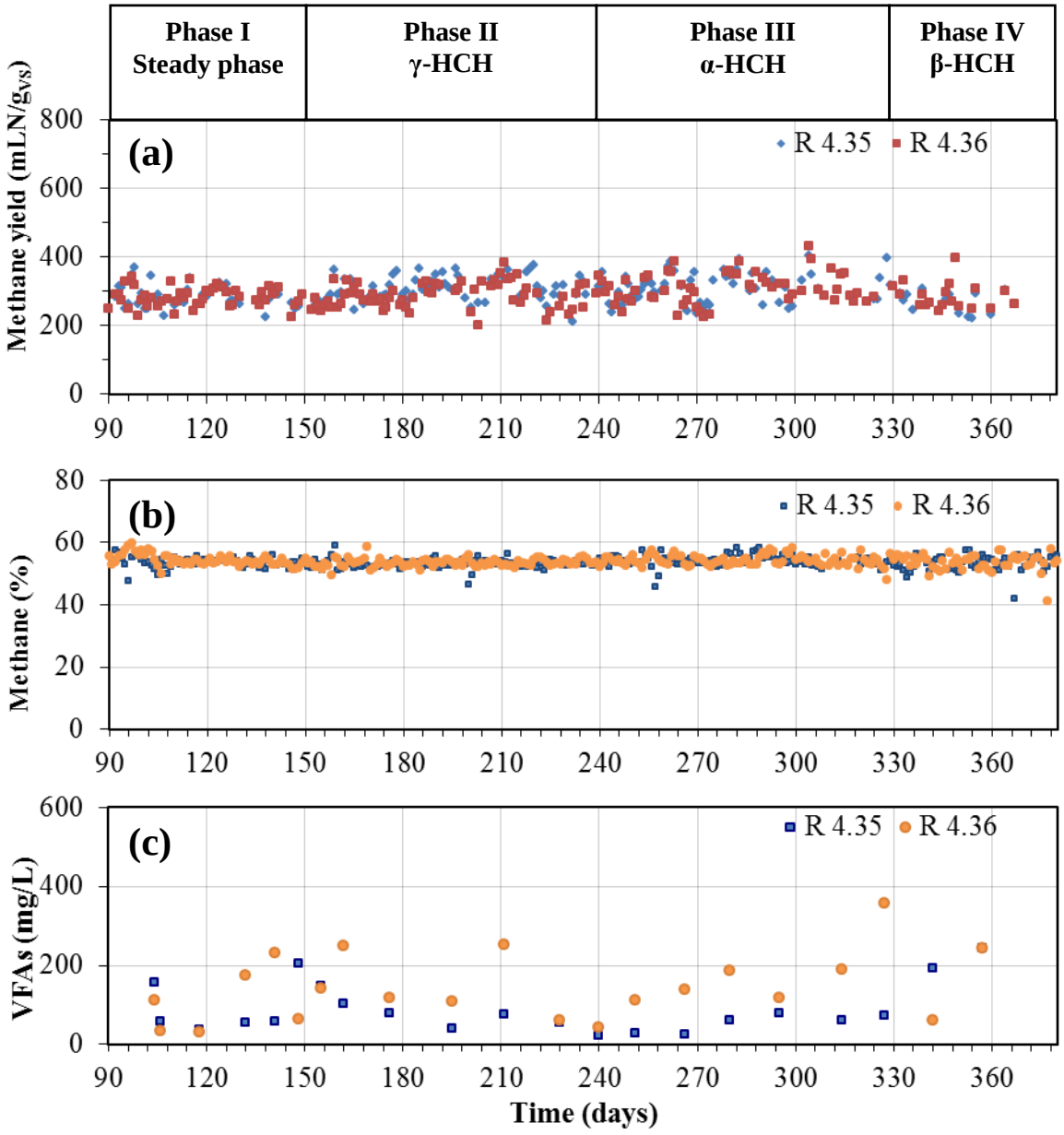

677

678 **Fig. 1** Methane yield (a), methane content (b) and total VFAs (c) in CSTRs over phases I to IV.

679 Data were corrected to pressure (101.325 kPa) and standard temperature (273.15 k), thus are

680 reported as normalized milliliters (mL_N) per gram of volatile solid (VS).

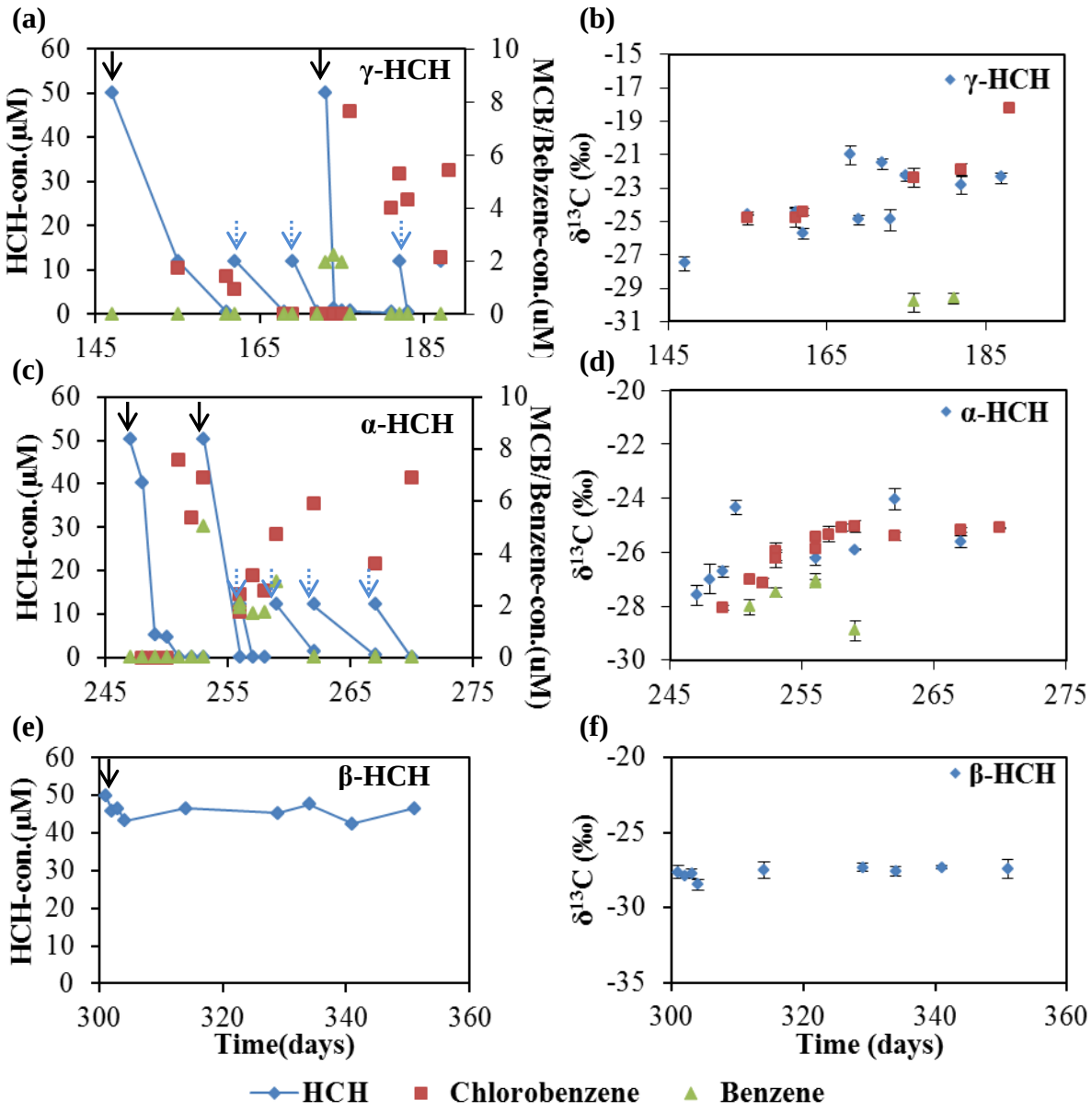

681 **Fig. 2** Concentrations and carbon isotope compositions of γ-HCH (a&b), α-HCH (c&d), β-HCH
682 (e&f) and metabolites (chlorobenzene and benzene). Values of 0 indicate that they were below
683 the detection limit. Black arrows mean adjustment of the concentration to 50 μM and blue
684 arrows represent the addition of HCH to 12 μM. Values of $\delta^{13}C$ are associated with
685 concentration and the data below the confidential interval of detection via GC-IRMS are not
686 shown here.

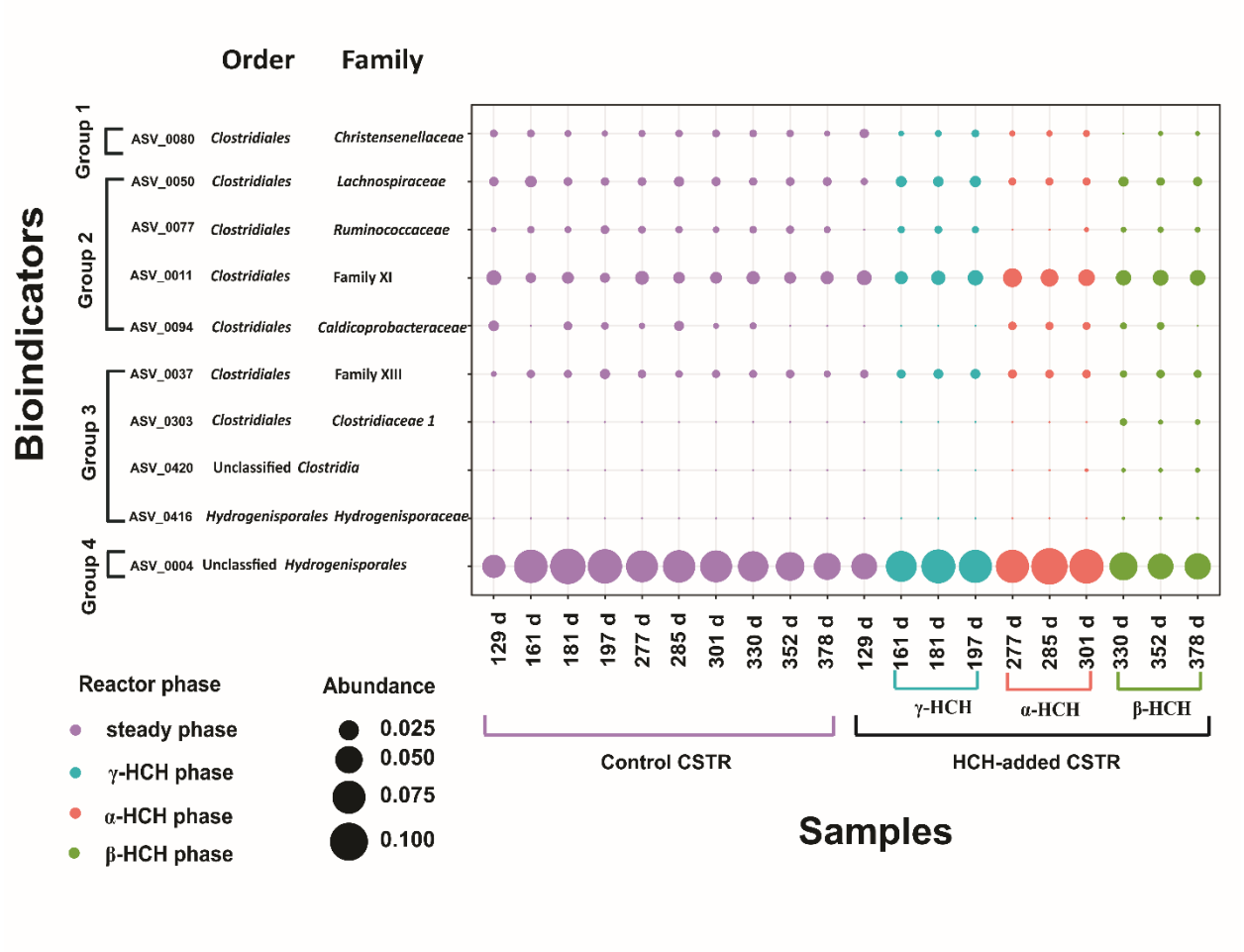

687

688 **Fig. 3** Relative abundance distribution of ASVs used as bioindicators in the control CSTR and

689 HCH-added CSTR.

690 ASVs separated in 4 different groups depending on statistic differences ($P < 0.05$) of abundance

691 using the LSMEANS test with FDR multiple correction, based on the interaction of pairwise

692 reactor phases: steady phase vs. β-HCH phase (Group1); γ-HCH phase vs. α-HCH phase

693 (Group2); γ-HCH phase vs. β-HCH phase (Group3); α-HCH phase vs. β-HCH phase (Group4).

694

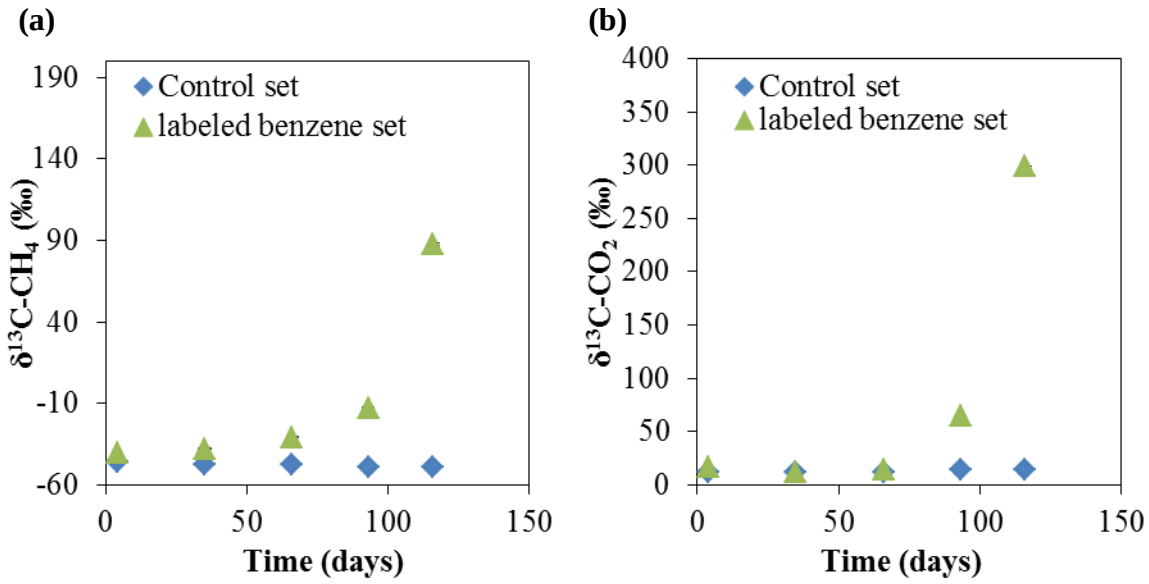

695

696 **Fig. 4** Carbon isotope signatures of methane (a) and CO_2 (b) in batch experiment with addition

697 of benzene-$^{13}C_6$.

698

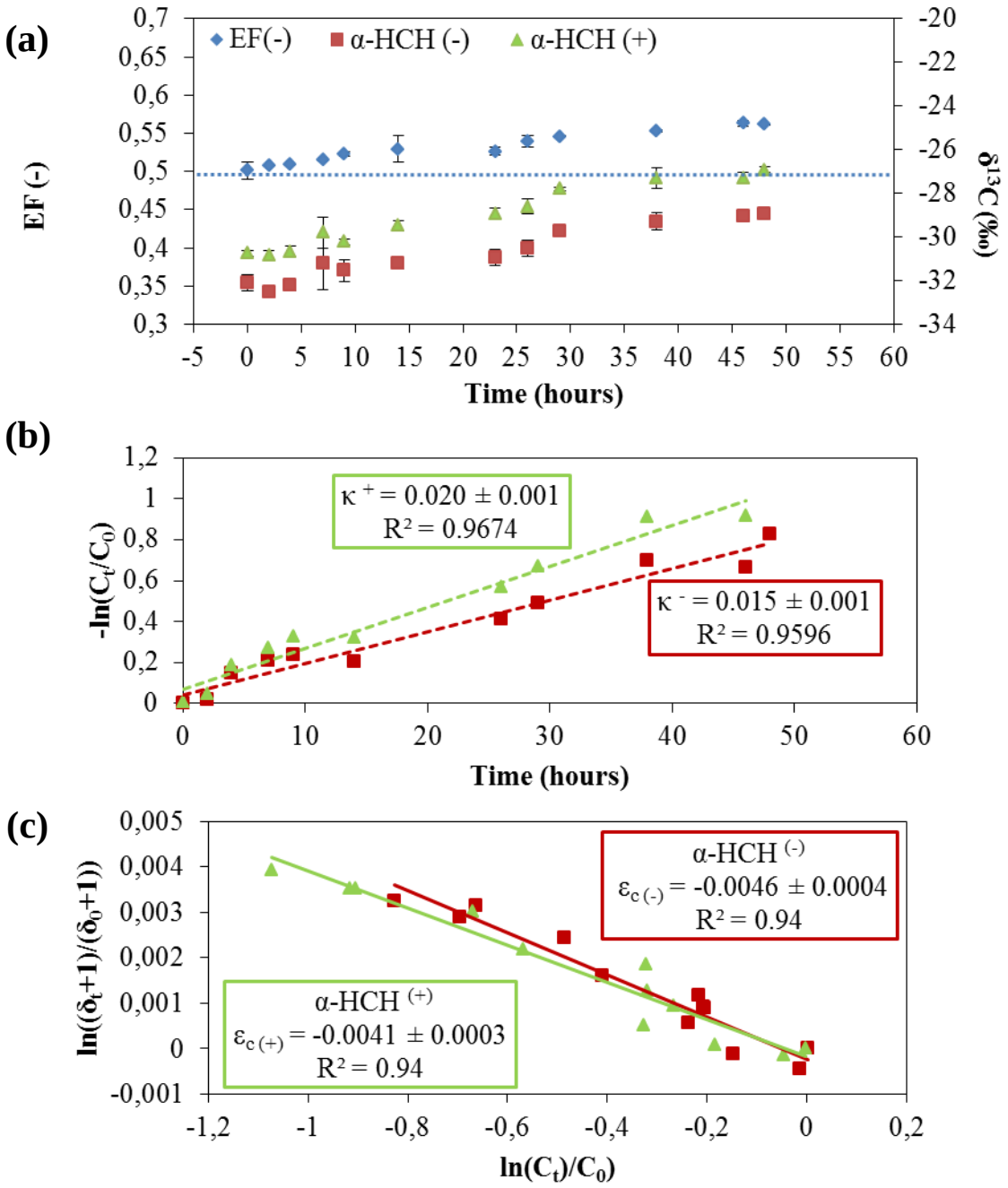

699 **Fig. 5** Enantiomer fractionation (EF) of (-) α-HCH and carbon isotope compositions of (-) / (+)

700 α-HCH in biogas slurry (batch experiment) (a)**;** the degradation kinetics of (-) α-HCH (◆) and

701 (+) α-HCH (■) in biogas slurry (b); carbon stable isotope enrichment factors of (-) / (+) α-HCH

702 (c).

703 **Scheme 1** Proposed interaction between anaerobic digestion and HCH dehalogenation with

704 subsequent mineralization

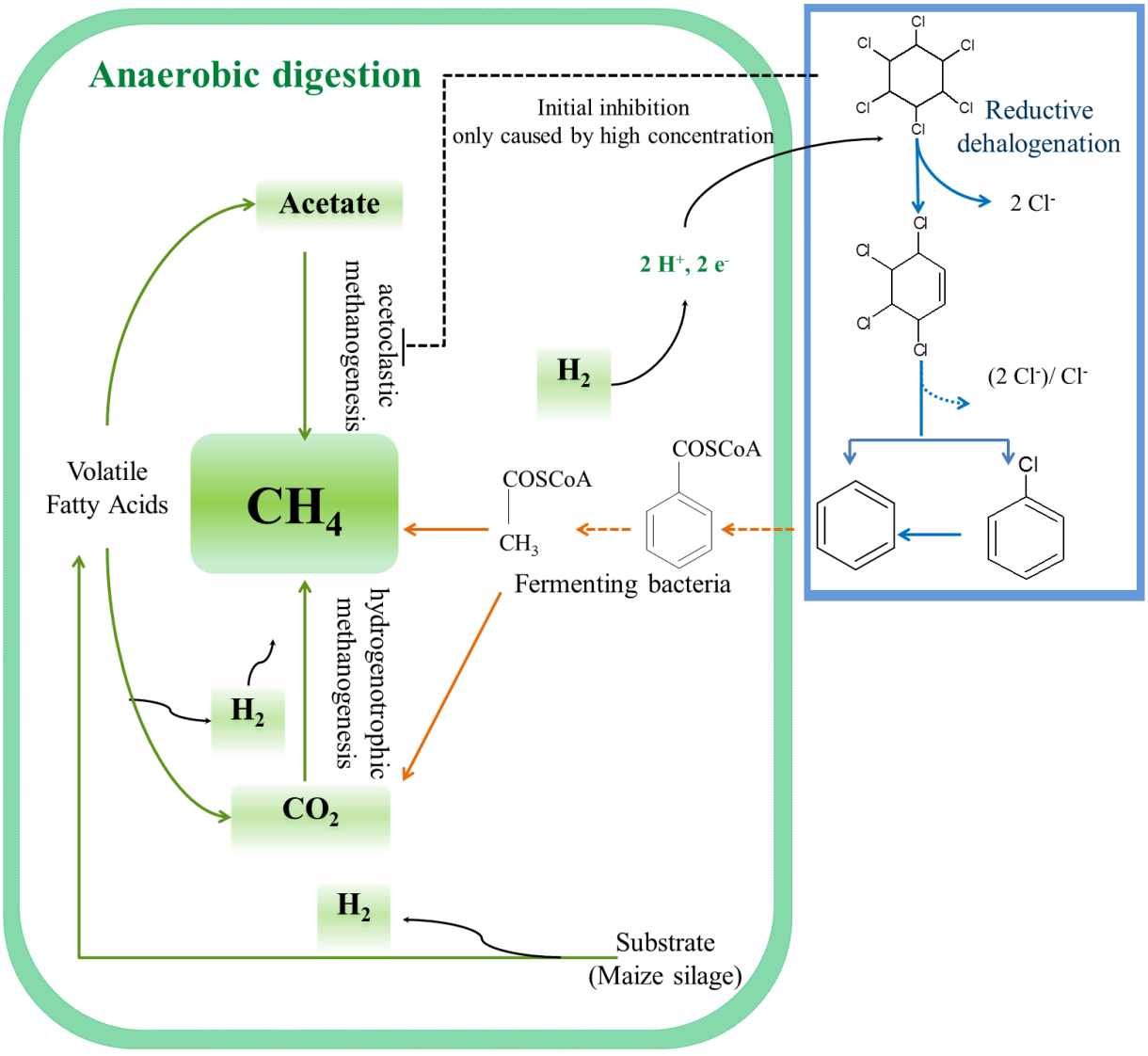

705

Supplementary Material A marked changes

Click here to download Supplementary Material: Appendix_A_Supplementary material-changes highlighted-18-09-2019_ur.docx

Abstract

Lindane, the γ-hexachlorocyclohexane (HCH) isomer, was among the most used pesticides worldwide. Although it was banned in 2009, residues of Lindane and other HCH-isomers are still found with high concentrations in contaminated fields. For clean-up, phytoremediation combined with anaerobic digestion (AD) of contaminated biomass to produce biogas and fertilizer could be a promising strategy and was tested in two 15 L laboratory-scale continuous-stirred-tank-reactors. During operation over one year by adding HCH isomers (γ, α and β) consecutively, no negative influence on conventional reactor parameters was observed. The γ- and α-HCH isomers were transformed to chlorobenzene and benzene, and transformation became faster along with time, while β-HCH was not removed. Genus *Methanosaeta* and order *Clostridiales,* showing significant enhancement on abundance with HCH addition, may be used as bioindicators for HCH dehalogenation in AD process. The potential for HCH degradation in AD system was restricted to axial Cl atoms of HCH and it showed slight enantioselective preference towards transformation of (+) α-HCH. Moreover, metabolite benzene was mineralized to CO_2 and methane, deducing from tracer experiments with benzene-$^{13}C_6$. Overall, AD appears to be a feasible option for treatment of γ and α-HCHs contaminated biomass.